

# Structurally Constrained Hybrid Derivatives Containing Octahydrobenzo[g or f]quinoline Moieties for Dopamine D2 and D3 Receptors: Binding Characterization at D2/D3 Receptors and Elucidation of a Pharmacophore Model

Dennis A. Brown,<sup>†</sup> Prashant S. Kharkar,<sup>†</sup> Ingrid Parrington,<sup>‡</sup> Maarten E. A. Reith,<sup>‡</sup> and Alope K. Dutta<sup>\*,†</sup>

Department of Pharmaceutical Sciences, Eugene Applebaum College of Pharmacy and Health Sciences, Wayne State University, Detroit, Michigan 48202, and Department of Psychiatry, Millhauser Laboratories, New York University School of Medicine, New York, New York 10016

Received July 13, 2008

A series of structurally constrained analogues based on hybrid compounds containing octahydrobenzo[g or f]quinoline moieties were designed, synthesized, and characterized for their binding to dopamine D2 and D3 receptors expressed in HEK-293 cells. Among the newly developed constrained molecules, *trans*-octahydrobenzo[f]quinolin-7-ol (**8**) exhibited the highest affinity for D2 and D3 receptors, the (–)-isomer being the eutomer. Interestingly, this hybrid constrained version **8** showed significant affinity over the corresponding nonhybrid version **1** (representing a constrained version of the aminotetralin structure only) when assayed under same conditions ( $K_i$  of 49.1 and 14.9 nM for **8** vs 380 and 96.0 nM for **1** at D2 and D3, respectively). Similar results were found with other lead hybrid compounds, indicating a contribution of the piperazine moiety in the observed enhanced affinity. On the basis of the data of new lead constrained derivatives and other lead hybrid derivatives developed by us, a unique pharmacophore model was proposed consisting of three pharmacophoric centers, two with aromatic/hydrophobic and one with cationic features.

## Introduction

The dopamine (DA<sup>a</sup>) receptor system has been aggressively targeted for drug development for the treatment of psychiatric illnesses, neurodegeneration, drug abuse, and other therapeutic areas.<sup>1,2</sup> The DA receptors, belonging to a class of G-protein-coupled receptors (GPCRs), are found in the central nervous system (CNS) and in the periphery.<sup>3</sup> In the CNS, DA receptors can be classified as being either D<sub>1</sub>-like or D<sub>2</sub>-like. The D<sub>1</sub>-like receptors include the D1 and D5 subtypes, and the D<sub>2</sub>-like receptors include the D2, D3, and D4 subtypes. These classifications are made on the basis of receptor pharmacology and function. Both D<sub>1</sub>-like and D<sub>2</sub>-like DA receptors share the same effector molecule, adenylate cyclase. Upon receptor activation, D<sub>1</sub>-like receptors activate adenylate cyclase whereas D<sub>2</sub>-like receptors inhibit it.<sup>4</sup>

An enormous amount of work has been done toward the development of DA agonists.<sup>5</sup> The initial research was focused on elucidating the bioactive conformation of the natural ligand, DA.<sup>6–10</sup> These efforts yielded the constrained class of compounds known as 2-aminotetralins, including (*S*)-(–)-5-hydroxy-2-(*N,N*-di-*n*-propylamino)tetralin [(*S*)-(–)-5-OH-DPAT] (Figure 1)<sup>6</sup> and (*R*)-(+)-7-hydroxy-2-(*N,N*-di-*n*-propylamino)tetralin [(*R*)-(+)-7-OH-DPAT] (Figure 1),<sup>11</sup> corresponding to the  $\alpha$ - and  $\beta$ -rotamers of DA, respectively. These studies revealed not only the bioactive conformation of the phenethyl side chain of DA but also that among the two hydroxyl groups in DA, the *m*-hydroxyl group is the most important in terms of receptor activation.<sup>6</sup> In regard to agonist interaction with the D2 and

D3 subtype receptors at the molecular level, a number of excellent studies with mutant D2 and D3 receptors have been published that delineated key binding residues in transmembrane domains 3, 5, and 7 for receptor activation.<sup>12–14</sup> Briefly, these studies indicated that two serine residues in TM-5 and one aspartate residue in TM-3 are critical for activation by agonists of both D2 and D3 receptors. The Asp110 residue in TM-3 has been shown to interact with the basic N-atom in DA and aminotetralin molecules. In these studies, Ser192 has been especially shown to be crucial for D3 interaction and activation. All these results suggest the existence of multiple bioactive conformations available for different agonists, resulting from different degrees of interactions with these key residues producing one signaling pathway.

The influence of the freely rotating amino group in 2-aminotetralins has been explored by introducing further conformational constraint into derived structures by the addition of another annulated ring, giving rise to monophenolic *cis*- and *trans*-1,2,3,4,4a,5,10,10a-octahydrobenzo[g]quinolines<sup>15</sup> and monophenolic *cis*- and *trans*-1,2,3,4,4a,5,6,10b-octahydrobenzo[f]quinolines.<sup>16</sup> Extensive SAR studies based on in vitro functional data have been conducted to determine the influence of hydroxyl group position, alkyl group chain length, and the geometry of ring fusion.<sup>15–19</sup> These studies showed that for phenolic 1,2,3,4,4a,5,10,10a-octahydrobenzo[g]quinolines and 1,2,3,4,4a,5,6,10b-octahydrobenzo[f]quinolines, only compounds having *trans* ring fusion were active (**1**, **2**, **3**, Figure 1)<sup>15,16</sup> and the corresponding *cis* analogues were almost completely inactive. This is largely attributed to the protonated amino group being unfavorably positioned to interact with the key aspartate residue in the *cis* conformation.<sup>15</sup> Compounds that showed activity in the functional assays had hydroxyl group substitution at either the 6 position [for benzo[g]quinolines (**2**, Figure 1)] or the 7/9 position for benzo[f]quinolines (**1** and **3**, Figure 1), corresponding to the  $\alpha$ - and  $\beta$ -rotameric forms, respectively.<sup>15,17a</sup> In this regard, it is important to mention that to the best of our

\* To whom correspondence should be addressed. Phone: 1-313-577-1064. Fax: 1-313-577-2033. E-mail: adutta@wayne.edu.

<sup>†</sup> Wayne State University.

<sup>‡</sup> New York University School of Medicine.

<sup>a</sup> Abbreviations: DA, dopamine; GPCR, G-protein-coupled receptor; CNS, central nervous system; MOE, Molecular Operating Environment; HEK, human embryonic kidney; 5-OH-DPAT, 5-hydroxy-2-(dipropylamino)tetralin; 7-OH-DPAT, 7-hydroxy-2-(dipropylamino)tetralin; PMA, phosphomolybdic acid.



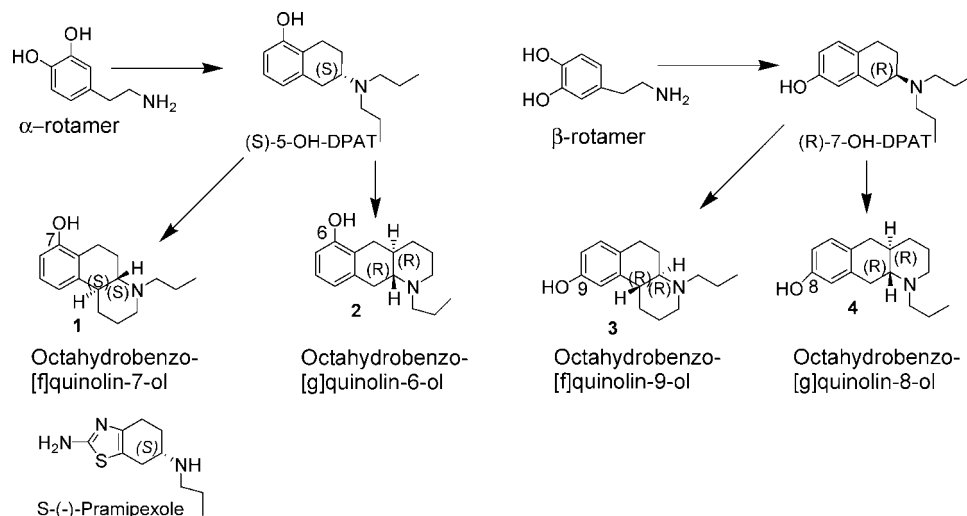


**Figure 1.** Molecular structures of dopamine D2/D3 receptor ligands.

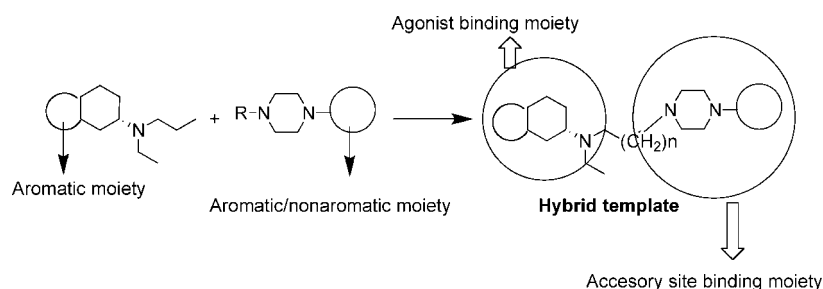


**Figure 2.** Hybrid template design.

knowledge no systematic receptor binding studies for DA receptor subtypes (D2 and D3) have been reported with these constrained derivatives, and hence, there is a lack of information on precise binding affinity of these derivatives with the respective receptor.

The effect of *N*-alkyl chain length on functional activity has also been investigated.<sup>15,16</sup> Linearly fused trans compounds with a hydroxyl group in the 6-position with alkyl groups *n*-propyl or smaller showed good functional activity. However, any compound containing an alkyl group larger than *n*-propyl was completely inactive, indicating the presence of a small alkyl-binding site in the receptor.<sup>15</sup> Also, all 8-hydroxy compounds (e.g., compound 4 in Figure 1) were inactive, regardless of alkyl substitution. Angularly fused compounds, e.g., 1 and 3, like their linear counterparts with 6-OH substitution, also showed functional activity. Interestingly, 7-OH angular compounds tolerated alkyl group size larger than *n*-propyl in functional assays. In fact, *n*-butyl or larger substitution showed enhanced affinity, showing that there is an additional "large" alkyl-binding site in D<sub>2</sub>-like DA receptors.<sup>10,15</sup> The relatively lower activity in octahydrobenzo[g]quinolinol series, compared to the octahydrobenzo[f]quinolinol series of compounds, was attributed to the unfavorable orientation of the nitrogen lone pair or protonated nitrogen atom and a sterically unfavorable orientation of the piperidine ring. Again, in all these studies, the precise nature of interaction was not available due to the lack of quantitative binding data for DA D2 and D3 receptor subtypes.

In an effort to develop novel, potent, and selective ligands for the DA D3 receptor subtype, our laboratory employed a hybrid structure approach, combining known DA agonist moieties with the *N*-arylpiperazine moiety derived from known D3 antagonists (Figure 2).<sup>20,21</sup> This approach was based on the

assumption that the aminotetralin moiety would interact with the agonist binding site in the DA receptor and the arylpiperazine fragment would interact with the accessory binding site residues in the D3 receptor to impart selectivity. Based on this approach, our group has been able to create highly potent DA D2/D3 agonists, with some compounds being very selective for the D3 receptor.<sup>21–23</sup> Compounds (–)-7 and 11 (Figure 3), two of our promising lead structures, exhibited high D3 selectivity in the functional assays and high *in vivo* potency in Parkinson's disease animal models.<sup>22,23</sup> In our effort to develop a pharmacophore model for our hybrid structures, we designed and synthesized a series of compounds that contain varying degrees of conformational constraint in the agonist moiety of the hybrid template. These compounds were then evaluated for their binding affinities at human D2L and D3 receptors in human embryonic kidney (HEK)-293 cell lines. Using molecular modeling approaches, we report in this paper the development of a three-point pharmacophore model for the binding of hybrid compounds to D2/D3 receptors.

## Chemistry

Scheme 1 outlines the synthesis of (±)-*cis*-1,2,3,4,4a,5,10,10a-octahydrobenzo[g]quinolin-8-ol derivatives. Amides 13a–c were prepared via condensation with appropriately substituted phenylpiperazines and chloroacyl chlorides in the presence of triethylamine. Originally, our aim was to synthesize only trans ring fused 1,2,3,4,4a,5,10,10a-octahydrobenzo[f] and [g]quinoline-8-ol molecules. When following the reported preparation procedure for *trans*-1,2,3,4,4a,5,10,10a-octahydrobenzo[g]quinoline,<sup>24</sup> we were unable to obtain the intermediate 8-methoxy-1,2,3,4,4a,5,10,10a-octahydrobenzo[g]quinoline in satisfactory yield, so we set out on devising an alternative synthesis. In the



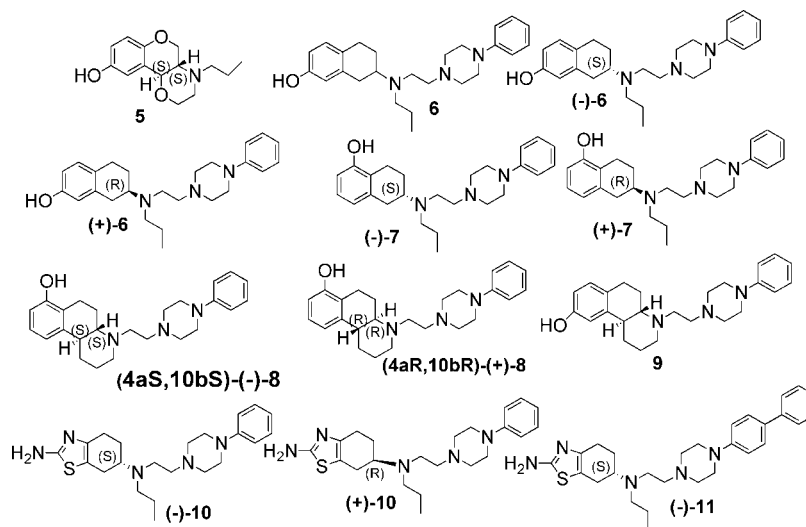


**Figure 3.** Molecular structures of compounds used for development of pharmacophore hypothesis.

first step, 3-methoxybenzyl bromide **14** was treated with activated zinc dust in THF to give zinc bromide **15**, which underwent a trans-metalation reaction with methyl 2-chloronicotinate in the presence of  $(\text{PPh}_3)_2\text{NiCl}_2$  to give intermediate **16**,<sup>25</sup> which was then reduced catalytically with  $\text{PtO}_2$  to yield substituted *cis*- and *trans*-piperidines **17**. The mixture of *cis*- and *trans*-isomers was not separated in the subsequent transformations. The amine **17** was then protected by conversion to its methyl carbamate. The ester was hydrolyzed by treatment with  $\text{LiOH}$  in  $\text{MeOH}/\text{H}_2\text{O}$ , and the resulting acid was converted to its acid chloride by reaction with  $\text{SOCl}_2$ . A Friedel–Crafts acylation reaction with  $\text{TiCl}_4$  was performed to yield benzylic ketone ( $\pm$ )-**19**. The ketone was reduced catalytically with  $\text{Pd/C}$  in the presence of perchloric acid, and then the carbamate was cleaved by treatment with hydrazine and  $\text{KOH}$  in ethylene glycol to give secondary amine ( $\pm$ )-**21**.

The relative stereochemical assignments of octahydrobenzoquinoline intermediates in this paper were made by converting the corresponding secondary amine intermediates, e.g., compound **21** in Scheme 1, to their *N*-benzyl analogues and observing the  $^1\text{H}$  NMR splitting pattern of the *N*-benzyl protons. It has been reported that the *N*-benzyl protons in *N*-benzyl substituted *cis*- and *trans*-fused octahydrobenzo[*f*] and *g*]quinolines appear as an AB quartet and that the chemical shift difference between the A and B portions differ between *cis*- and *trans*-fused compounds.<sup>26</sup> The observed chemical shift difference for *cis*-fused compounds is around 0.6  $\delta$  ppm, whereas the difference for the *trans*-fused counterparts is much larger, around 0.9–1.0  $\delta$  ppm. The chemical shift differences of our synthesized compounds are in accordance with these reported values (see the Supporting Information for the syntheses and NMR data for *N*-benzyl compounds).

Amine ( $\pm$ )-**21** was condensed with chlorides **13a** and **13b** to give amides ( $\pm$ )-**22a,b**, respectively. The amide carbonyls were then reduced with  $\text{LiAlH}_4$  to provide **23a,b**. Demethylation of methyl ethers by  $\text{BBr}_3$  in  $\text{CH}_2\text{Cl}_2$  gave the final compounds ( $\pm$ )-**24a,b**.

The second attempt to synthesize ( $\pm$ )-*trans*-1,2,3,4,4a,5,10,10a-octahydrobenzo[*g*]quinoline derivatives is described in Scheme 2. The first aim of this synthesis was to selectively alkylate position 1 of 7-methoxy-2-tetralone **25**. This was accomplished by converting **25** to its enolate with  $\text{NaH}$  followed by trapping with dimethyl carbonate to give compound **26**.<sup>27</sup> This was then converted to its dianion with  $\text{LDA}$  and treated with chloropro-

pionitrile to give **27**. This ester was decarboxylated in the presence of  $\text{LiCl}$  and  $\text{H}_2\text{O}$  in  $\text{DMSO}$  to yield ketone **28**, which was then protected by conversion to acetal. The cyano group was reduced in the presence of Raney  $\text{Ni}$  to give amine **30**, which was then treated with  $\text{HCl}/\text{MeOH}$  to give iminium **31**. The second aim of this synthesis was accomplished by controlling the stereoselectivity of iminium reduction of **31** by using  $\text{NaCNBH}_3$ . The *trans*-fused secondary amine ( $\pm$ )-**32** was the major product detected (stereochemistry assigned based on the *N*-benzyl method).<sup>26</sup> Amine ( $\pm$ )-**32** was alkylated with **13a–c** to yield amides ( $\pm$ )-**33a–c**. These amides were reduced and demethylated in the same manner as described above to produce targets ( $\pm$ )-**35a–c**.

Scheme 3 outlines the synthesis of ( $\pm$ )-*trans*-1,2,3,4,4a,5,6,10b-octahydrobenzo[*f*]quinolin-7-ol derivatives. Amine ( $\pm$ )-**36** was synthesized as previously described.<sup>28</sup> Racemic **37** was prepared by *N*-alkylating ( $\pm$ )-**36** with chloride **13a** to give amide ( $\pm$ )-**37**, which was then reduced and demethylated to give ( $\pm$ )-**8**. Compound ( $\pm$ )-**36** was next resolved into its enantiomers by following the procedure described by Wikström et al.<sup>16</sup> as shown in Scheme 4. Experimental details for separation of enantiomers are provided in the Supporting Information. Compounds (+)-**8** and (–)-**8** were obtained by following the same procedure as for the racemic version. Compound ( $\pm$ )-*trans*-4-propyl-1,2,3,4,4a,5,6,10b-octahydrobenzo[*f*]quinolin-7-ol (**1**) was also synthesized from amine ( $\pm$ )-**36** as a reference compound.

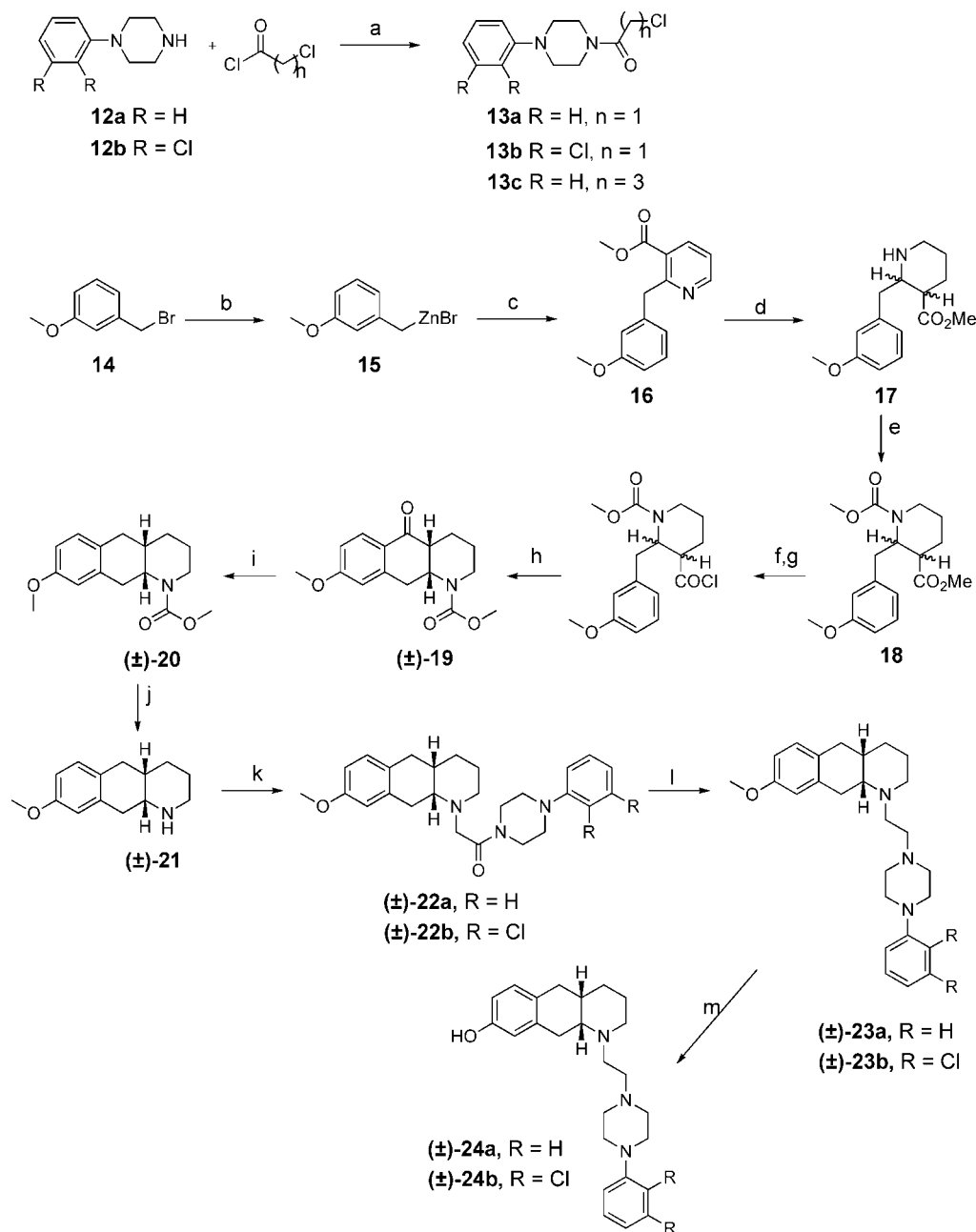
Scheme 5 outlines the synthesis of ( $\pm$ )-*trans*-1,2,3,4,4a,5,10,10a-octahydrobenzo[*g*]quinolin-6-ol derivatives. Secondary amine **40** was prepared as previously described.<sup>29</sup> Completion of the syntheses of ( $\pm$ )-**43a,b** was carried out in a similar manner as described for the previous compounds. The reference compound **2** was also synthesized from amine intermediate **40**.

In addition, the synthesis of (–)-5-OH-DPAT, (–)-**6**, and racemic **9** were also carried out to use them as reference compound and in our SAR studies. The detailed synthesis of **9** is given in the Supporting Information.

## Results and Discussion

Our previous articles on hybrid drug development approach for D2/D3 receptors outlined the development of aminotetralin-arylpiperazine-based compounds exhibiting D3 preferential activity both in binding and in functional assays.<sup>22,23</sup> One of the very first compounds based on this hybrid template was



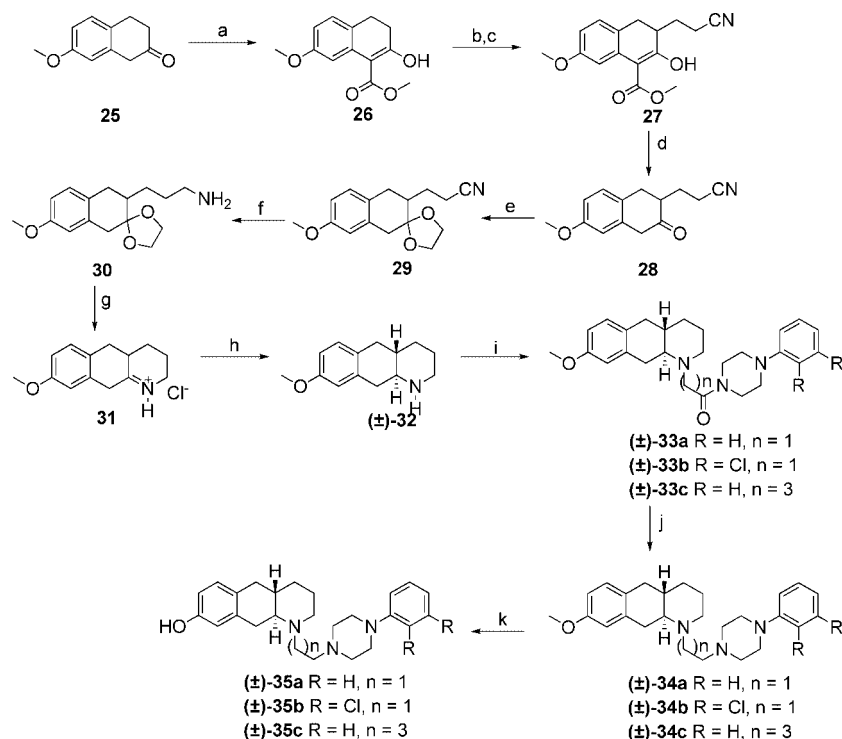
Scheme 1<sup>a</sup>

<sup>a</sup> Reagents and conditions: (a) Et<sub>3</sub>N, CH<sub>2</sub>Cl<sub>2</sub>, 0 °C; (b) Zn dust, THF, 0 °C; (c) methyl 2-chloronicotinate, (PPh<sub>3</sub>)<sub>2</sub>NiCl<sub>2</sub>, THF; (d) (i) HCl, Et<sub>2</sub>O; (ii) PtO<sub>2</sub>, MeOH; (e) methyl chloroformate, K<sub>2</sub>CO<sub>3</sub>, CH<sub>2</sub>Cl<sub>2</sub>; (f) LiOH, MeOH, H<sub>2</sub>O; (g) SOCl<sub>2</sub>, CH<sub>2</sub>Cl<sub>2</sub>, cat. DMF; (h) TiCl<sub>4</sub>, CH<sub>2</sub>Cl<sub>2</sub>, 0 °C; (i) NH<sub>2</sub>NH<sub>2</sub>, KOH, H<sub>2</sub>O, (CH<sub>2</sub>OH)<sub>2</sub>, reflux; (k) **13a/b**, K<sub>2</sub>CO<sub>3</sub>, CH<sub>3</sub>CN; (l) LiAlH<sub>4</sub>, THF, reflux; (m) BBr<sub>3</sub>, CH<sub>2</sub>Cl<sub>2</sub>, -78 °C.

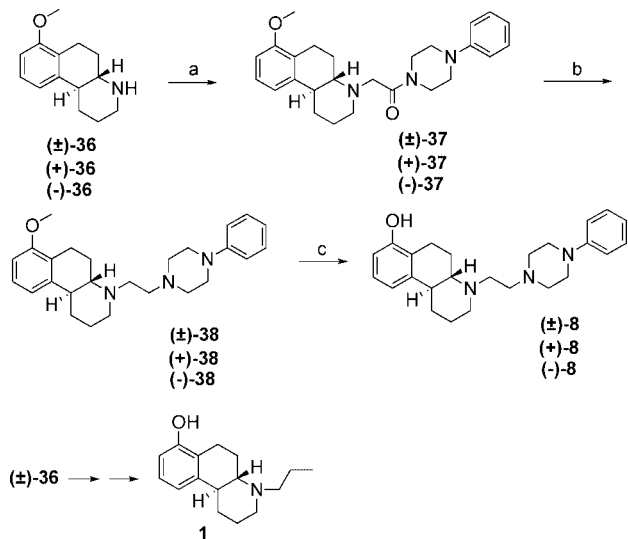
compound **6** and its corresponding enantiomers (–)-**6** and (+)-**6**. The initial D2/D3 binding data demonstrated very little difference in affinity between these two enantiomers. However, we recently realized that during the process of separation of these two enantiomers, we inadvertently converted most of the compounds back to its racemic version, and thus, the binding data were erroneous. A newer approach to separate these enantiomers has been adopted by us recently that gave us the two enantiomers with high enantiomeric purity.<sup>22,30</sup> The new data show appreciable differences between the two enantiomers, with the (+)-(*R*)-**6** isomer expectedly showing the highest affinity for the both D2 and D3 receptors. This is in line with the binding data of the corresponding enantiomers of the parent structure 7-OH-DPAT. Thus, the enantiomers (–)-**6** and (+)-**6** (Figure 3) possessed higher binding affinity for D3 receptors and lower binding affinity for D2 receptors (*K*<sub>i</sub> of 38.6 and 1.77

nM for D3 and *K*<sub>i</sub> of 809 and 40.6 nM for D2). A similar trend was observed for the hybrid structures derived from 5-OH-DPAT, compounds (–)-**7** and (+)-**7** (Figure 3). The observed differences in the inhibition constants for (–)-**7** and its enantiomer (+)-**7** were ~20-fold for the D3 receptor (18.4 nM versus 0.82 nM) and ~9-fold for the D2L receptor (238 nM versus 26 nM).<sup>22</sup> These data are also in line with the data found from 5-OH-DPAT affinity. However, compound (–)-**7** exhibited more than 4-fold higher affinity compared to (–)-5-OH-DPAT under our binding assay conditions for both the D2 and D3 receptors (*K*<sub>i</sub> of 26 vs 220 nM for D2 and *K*<sub>i</sub> of 0.82 vs 4.73 nM for D3, respectively). This is an interesting finding, since it indicates that the presence of the piperazine moiety further enhanced the affinity of this hybrid compound while maintaining its strong agonist activity.<sup>22</sup> Thus, contribution of piperazine fragment increased the interaction with the D2/D3 receptors.



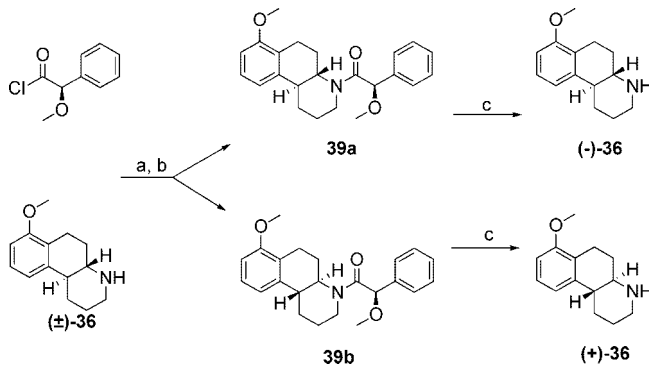
Scheme 2<sup>a</sup>

<sup>a</sup> Reagents and conditions: (a) NaH, PhCH<sub>3</sub>, dimethyl carbonate, reflux; (b) 2 equiv of LDA, THF, -78 °C; (c) bromopropionitrile; (d) LiCl, H<sub>2</sub>O, DMSO, reflux; (e) (CH<sub>2</sub>OH)<sub>2</sub>, TsOH, triethyl orthoformate, CH<sub>2</sub>Cl<sub>2</sub>; (f) Raney Ni, MeOH; (g) 6 M HCl, MeOH, reflux; (h) NaCNBH<sub>3</sub>, MeOH; (i) **13a**/**13b**/**13c**, K<sub>2</sub>CO<sub>3</sub>, CH<sub>3</sub>CN, cat. KI, reflux; (j) LiAlH<sub>4</sub>, THF, reflux; (k) BBr<sub>3</sub>, CH<sub>2</sub>Cl<sub>2</sub>, -78 °C.

Scheme 3<sup>a</sup>

<sup>a</sup> Reagents and conditions: (a) **13a**, K<sub>2</sub>CO<sub>3</sub>, CH<sub>3</sub>CN, reflux; (b) LiAlH<sub>4</sub> (c) BBr<sub>3</sub>, CH<sub>2</sub>Cl<sub>2</sub>, -78 °C.

Monophenolic *cis*- and *trans*-1,2,3,4,4a,5,10,10a-octahydrobenzo[g]quinolines had been evaluated for interactions with D<sub>1</sub>-like and D<sub>2</sub>-like dopamine receptors and compared with the effects of the corresponding unconstrained aminotetralins a couple of decades ago.<sup>15</sup> These molecules were mainly evaluated for functional activity in the membrane preparations. Similarly, *cis*- and *trans*-1,2,3,4,4a,5,6,10b-octahydrobenzo[f]quinolines were tested for central DA and serotonin receptor-stimulating activity using biochemical and behavioral tests in rats.<sup>15,16</sup> With the availability of cloned DA receptor subtypes, it is now possible to investigate the affinity and selectivity of these compounds for DA receptor subtypes, which was not possible

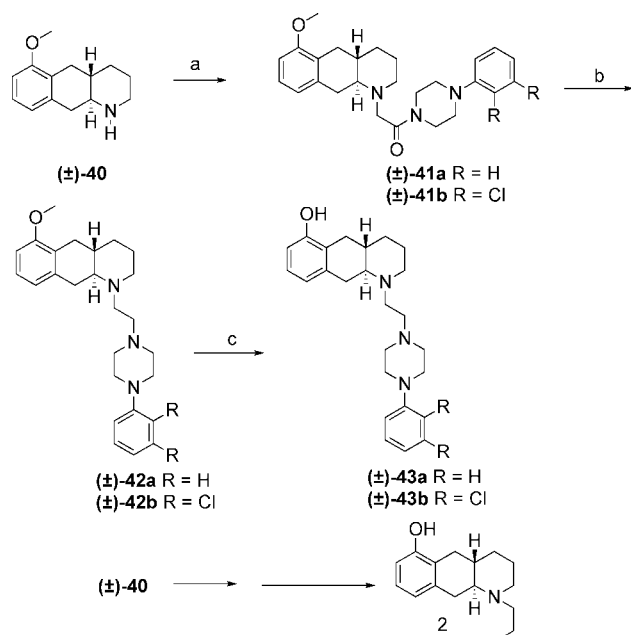
Scheme 4<sup>a</sup>

<sup>a</sup> Reagents and conditions: (a) NaOH, H<sub>2</sub>O/CH<sub>2</sub>Cl<sub>2</sub>; (b) crystallization followed by HPLC; (c) (i) Na *tert*-butoxide, H<sub>2</sub>O, THF; (ii) HCl, MeOH.

earlier. With this background, it was of interest to us to apply the hybrid structure approach to these octahydrobenzo[f]- and [g]quinolines to investigate the following goals: (1) evaluate binding affinity for the DA receptor subtypes with the aim of delineating the factors responsible for the observed trend in binding affinity and D<sub>2</sub>/D<sub>3</sub> selectivity, if any, in these derivatives and (2) develop a pharmacophore model for our hybrid derivatives by using these conformationally constrained DA analogues including aminotetralins.

The binding data of the target compounds for DA D<sub>2</sub> and D<sub>3</sub> receptors are given in Table 1. In the case of hybrid (±)-*trans*-1,2,3,4,4a,5,10,10a-octahydrobenzo[g]quinolin-6-ol derivatives, represented by compound (±)-**43a**, the binding affinities for the D<sub>3</sub> and D<sub>2</sub> receptors (*K*<sub>i</sub>(D<sub>3</sub>) = 736 and *K*<sub>i</sub>(D<sub>2</sub>) = 1712 nM) were found to be low. The corresponding *N*-*n*-propyl analogue **2** (Figure 1), of the parent structure of **43a**, was reported to be active for the DA receptors in functional assays.<sup>15</sup> However, the *cis*-analogues of **2** were reported to be



Scheme 5<sup>a</sup>

<sup>a</sup> Reagents and conditions: (a) **13a/b**, K<sub>2</sub>CO<sub>3</sub>, CH<sub>3</sub>CN, reflux; (b) LiAlH<sub>4</sub>, THF, reflux; (c) BBr<sub>3</sub>, CH<sub>2</sub>Cl<sub>2</sub>, -78°C.

**Table 1.** Affinity for Cloned D<sub>2L</sub> and D<sub>3</sub> Receptors Expressed in HEK Cells Measured by Inhibition of [<sup>3</sup>H]Spiperone Binding<sup>a</sup>

compd	K <sub>i</sub> (nM)		D <sub>2L</sub> /D <sub>3</sub>
	D <sub>2L</sub> [ <sup>3</sup> H]spiperone	D <sub>3</sub> [ <sup>3</sup> H]spiperone	
(±)-7-OH-DPAT	311 ± 47	6.19 ± 1.4	50.2
(-)-5-OH-DPAT	220 ± 37.7	4.73 ± 0.64	46.5
<b>2</b>	2780 ± 457	395 ± 75	7.03
<b>1</b>	347 ± 51	96.0 ± 4.7	3.61
(-)- <b>6</b>	809 ± 65	38.6 ± 0.7	21
(+)- <b>6</b>	40.6 ± 3.6	1.77 ± 0.42	22.9
(-)- <b>7</b>	26.0 ± 7.5	0.825 ± 0.136	31.5
(+)- <b>7</b>	238 ± 14	18.4 ± 1.0	12.9
<b>9</b>	219 ± 30	72.2 ± 17.2	3
(-)- <b>10</b>	243 ± 65	4.15 ± 0.76	58.6
(+)- <b>10</b>	1979 ± 567	44.0 ± 10.6	45.0
<b>11</b>	234 ± 40	0.925 ± 0.234	253
(±)- <b>24a</b>	3326 ± 788	419 ± 119	7.94
(±)- <b>24b</b>	148 ± 30	187 ± 24	0.79
(±)- <b>35a</b>	2522 ± 554	473 ± 167	5.33
(±)- <b>35b</b>	338 ± 35	256 ± 69	1.3
(±)- <b>35c</b>	289 ± 56	102 ± 20	2.83
(±)- <b>8</b>	49.1 ± 10.3	14.9 ± 4.3	3.30
(+)- <b>8</b>	835 ± 182	89.3 ± 19.4	9.35
(-)- <b>8</b>	23.6 ± 1.1	4.95 ± 1.08	4.77
(±)- <b>43a</b>	1712 ± 355	736 ± 206	2.33
(±)- <b>43b</b>	136 ± 23	168 ± 24	0.80

<sup>a</sup> Results are mean values ± SEM for three to eight experiments each performed in triplicate.

inactive. Also, the transition from *n*-propyl to *n*-butyl led to complete loss of functional activity for the racemate of **2**.<sup>15</sup> Since no binding data were available for interaction of this compound **2** with DA receptors, this compound was resynthesized by us to evaluate its binding interaction with the cloned DA receptor subtypes. As shown in Table 1, compound **2** exhibited very poor affinity for both D<sub>2</sub> and D<sub>3</sub> receptors. Thus, the data from the hybrid structure (±)-**43a** correlated well with the binding affinity for the nonhybrid structure. No attempts were made to synthesize cis-analogues of **43a**. However, the dichloro derivative **43b** was significantly more potent and the effect was more significant for D<sub>2</sub> receptor compared to D<sub>3</sub> receptor. Thus, **43b** was 12

times more potent at D<sub>2</sub> compared to **43a** and 4-fold more potent at D<sub>3</sub> compared to **43a** (*K<sub>i</sub>* of 136 nM vs 1712 nM, respectively).

In the case of (±)-*cis*- and (±)-*trans*-1,2,3,4,4a,5,10,10a-octahydrobenzo[*g*]quinolin-8-ol hybrid derivatives, represented by compounds (±)-**24a,b** and (±)-**35a–c**, respectively, a similar trend was observed when compared to their corresponding 6-OH analogues (**43a,b**). Previously, all 8-OH *N*-*n*-propyl derivatives were reported to be inactive in DA receptor functional assays.<sup>15</sup> Compound (±)-**24a**, a *cis* derivative, exhibited very weak binding affinity at D<sub>3</sub> receptor (*K<sub>i</sub>* = 419 nM) and even weaker affinity for the D<sub>2</sub> receptor (*K<sub>i</sub>* = 3326 nM). As seen with **43b**, the corresponding dichloro analogue **24b** improved the affinity to a great extent, which can be attributed to the presence of 3,4-dichloro group possibly promoting hydrophobic interactions with the DA receptors. This phenomenon was observed with other known DA receptor ligands as well. A similar trend was observed for the *trans* compounds (±)-**35a** and (±)-**35b**. The *trans* compounds (±)-**35b** and (±)-**35c** were found to possess moderate affinity for the D<sub>3</sub> receptor (Table 1). A change of spacer length between the octahydrobenzo[*g*]quinoline and the piperazine moieties from 2 to 4, as depicted in **35a** and **35c**, led to ~3-fold gain in affinity for the D<sub>3</sub> and ~9-fold for the D<sub>2</sub> receptors (*K<sub>i</sub>* of 473 vs 102 nM for D<sub>3</sub> and *K<sub>i</sub>* of 2522 vs 289 nM for D<sub>2</sub>, respectively) for **35c**. These benzo[*g*]quinoline derivatives exhibited moderate selectivity for the DA D<sub>3</sub> receptor subtypes.

Having investigated the benzo[*g*]quinolines, we started analyzing the binding data for the hybrid 1,2,3,4,4a,5,6,10b-octahydrobenzo[*f*]quinolin-7-ol and -9-ol derivatives. The most active compound in the present study was (±)-**8** (*K<sub>i</sub>*(D<sub>3</sub>) = 14.9 nM, *K<sub>i</sub>*(D<sub>2</sub>) = 49.1 nM, respectively), which belongs to the 7-hydroxy series; the corresponding 9-OH compound **9** (Figure 3), which was synthesized by us, exhibited moderate affinity for the D<sub>3</sub> receptor (*K<sub>i</sub>*(D<sub>3</sub>) = 72 nM, *K<sub>i</sub>*(D<sub>2</sub>) = 219 nM). Even though the compound (±)-**8** possessed higher potency, it lacked high selectivity for the D<sub>3</sub> receptor (Table 1). The *trans*-7-hydroxy-*N*-*n*-propyl derivatives were reported to be more active than their *cis* counterparts in this structural class.<sup>17a</sup> Also, the change from *n*-propyl to *n*-butyl substitution was reported to increase activity. We further resolved (±)-**8** and tested their binding affinities. Thus, in accordance with what has been previously reported,<sup>21</sup> we observed higher binding affinity in the (-)-**8** isomer (corresponding to (4*aS*,10*bS*) configuration) (Table 1). It is again important to point out here that complete binding characterization of the parent compound **1** and its analogues for D<sub>2</sub>/D<sub>3</sub> receptors was never carried out. In agreement with the higher binding affinity of (-)-**7** (hybrid structure based on (*S*)-(-)-5-OH-DPAT) compared to its enantiomer, a good separation of affinity was found for the D<sub>3</sub> and D<sub>2</sub> receptors in (+)-**8** and (-)-**8** (*K<sub>i</sub>* of 89.3 and 4.95 nM for D<sub>3</sub> and *K<sub>i</sub>* of 835 and 23.6 nM for D<sub>2</sub> receptor, Table 1). In order to judge correctly the impact of the hybrid version of 1,2,3,4,4a,5,6,10b-octahydrobenzo[*f*]quinolin-7-ol derivatives in binding, we synthesized and characterized the corresponding nonhybrid derivative **1** to evaluate its binding affinity for the D<sub>2</sub>/D<sub>3</sub> receptors. Interestingly, as observed in the case of (-)-5-OH-DPAT and (-)-**7**, the hybrid racemic version (±)-**8** exhibited more than 6-fold affinity compared to **1** (*K<sub>i</sub>* of 14.9 vs 96 nM for D<sub>3</sub> and *K<sub>i</sub>* of 49 vs 380 nM for D<sub>2</sub>, respectively, Table 1). This again demonstrated the unique contribution of the piperazine fragment in enhancing affinity of hybrid compounds compared to known ligands. Interestingly, hybrid constrained derivatives did not contain any free *N*-alkyl group, unlike nonhybrid constrained versions, which displayed an



influence of nature of *N*-alkyl substitution on activity.<sup>15,17a</sup> The fact that an alkyl group could be replaced by a substituted piperazine fragment with enhancement of binding activity may indicate development of additional cooperative binding interactions of the hybrid derivatives with D2/D3 receptors.

The data taken together represent our SAR study with hybrid derivatives developed for D2/D3 receptors to understand the molecular mode of interactions and to derive a pharmacophore model. Thus, we designed and synthesized conformationally constrained versions in which the aminotetralin moiety was converted into *trans*-1,2,3,4,4a,5,10,10a-octahydrobenzo[*g*]quinoline and *trans*-1,2,3,4,4a,5,6,10b-octahydrobenzo[*f*]quinoline structures. Hybrid compounds with a *trans*-1,2,3,4,4a,5,6,10b-octahydrobenzo[*f*]quinoline structure exhibited more affinity for D2/D3 receptors than those with a *trans*-1,2,3,4,4a,5,10,10a-octahydrobenzo[*g*]quinoline, indicating preference for one constrained conformation over the other. Overall, hybrid derivatives exhibited a significant increase of affinity compared to the corresponding nonhybrid counterparts, reflecting an important role of the piperazine moiety in affinity for dopamine receptors. Having acquired all the necessary data, our next task was to carry out a computational analysis to derive a reliable pharmacophore model of hybrid compounds for their binding to D2/D3 receptors.

Next, we extended our studies toward the generation of pharmacophore hypotheses based on these conformationally constrained bi- and tricyclic hybrid structures. There are few reports of DA receptor pharmacophoric requirements based on various ligands including conformationally constrained tricyclic aminotetralins.<sup>15–17a</sup> The central theme of these receptor models was the importance of various positions taken by the *N*-substituents. One orientation disfavored any groups bigger than *n*-propyl (sterically defined), whereas other orientations tolerated bigger groups (e.g., McDermed's DA-receptor model,<sup>15</sup> Wikström's extended model<sup>16</sup>) (sterically favorable). The hybrid compounds (linear and angular) described in the present investigation follow the general requirements depicted by above-mentioned DA-receptor models. For additional description and illustration with the help of representative hybrid compounds of this DA-receptor model, readers are encouraged to see the Supporting Information.

In the initial trial runs of pharmacophore generation with the known D2/D3 ligands (*S*)-5-OH-DPAT, *R*-(+)-7-OH-DPAT, and **5** (*R*-(+)-PD128907)<sup>17b</sup> (Figure 1), the best three-point pharmacophore (based on overall alignment score), as depicted in Figure 4a, shows the presence of one aromatic/hydrophobic feature occupied by the aromatic ring (green), another hydrophobic feature present near the *N*-*n*-propyl groups (green) common to all three ligands, and the quaternary N as the cationic feature (blue). Shown as purple are the two features depicting the directions of the phenolic hydroxyl H-bond donor and the H attached to cationic N (required for reinforced H-bonding). Figure 4a clearly shows the orientation of the H atom attached to cationic N in the direction of the purple sphere, representing a possible interaction with the Asp residue in TM-3. Similarly, another purple sphere located near phenolic hydroxyls represents the Ser residue(s) of the DA receptor subtypes. The distance between the aromatic/hydrophobic feature near the aromatic ring and the cationic N was found in the narrow range of 5.06–5.16 Å. This distance falls within the range of 4.1–6.1 Å reported for the same interfeature distance in a pharmacophore derived from known D3 ligands.<sup>31</sup>

A pharmacophore model was generated on the basis of the hybrid compounds (+)-**6** and (–)-**7**, representing bicyclic hybrid

aminotetralins structures, along with (–)-**8**, a hybrid tricyclic aminotetralin, and (–)-**11**, representing a 2-aminothiazole-based fused bicyclic system. Of the several pharmacophore hypotheses generated, two representative hypotheses were selected on the basis of the overall alignment score, nature of features present, and the molecules covered. Only the top ranked of the two hypotheses is shown in Figure 4b along with the hybrid analogues aligned onto these features. These two hypotheses differ in interfeature distances as shown in Figure 4c, which depicts the features and the corresponding interfeature distance ranges. The range of distances results from changes in the conformation of the ethylene bridge connecting the cationic N with the arylpiperazine portion. In Figure 4b, this ethylene linker adopted the gauche conformation whereas in the second hypothesis (not shown), it adopted the anti conformation. These interfeature distances are shown in Table 2. These distances were measured from the gauche and anti conformations of the individual molecules, whereas interfeature distance ranges shown in Figure 4c were measured from the individual pharmacophore hypotheses (representing gauche and anti conformations of the ethylene bridge). The distances between hydrophobic features with one centered on the aminotetralin aryl portion (Ar<sup>1</sup>) and the other on the phenyl ring of arylpiperazine portion (Ar<sup>2</sup>), as well as the distances between cationic N and the arylpiperazine hydrophobic features, were greater in the case of the anti conformation (Table 2). The distances between the cationic N and Ar<sup>1</sup> were reduced in the case of the anti conformation compared to the gauche conformation (shown in Figure 4b). We strongly believe that these conformations and the associated interfeature distances coupled with other factors govern the selectivity for D2/D3, provided the above-mentioned features (shown in Figure 4b) are present in the molecules. Figure 4b represents the DA receptor (D2 and D3) ligand pharmacophore depicting three features consisting of two aromatic/hydrophobic and one cationic feature. Along with these three features, it shows the Don2 feature, which represents the direction in which the H-bond donor attached to the aromatic portion should be oriented for optimal interaction with the receptor(s). The aromatic/hydrophobic features represent (1) Ar<sup>1</sup>, the phenyl ring in hybrid aminotetralins (+)-**6**, (–)-**7**, and (–)-**8** and 2-aminothiazole ring in (–)-**11**, and (2) Ar<sup>2</sup>, the phenyl ring attached to N-4 of piperazine. One set of aromatic/hydrophobic and cationic features is common to parts a and b of Figure 4. This set of two features is similar to that described for the D3 ligand pharmacophore by Varady, et al.<sup>31</sup> However, compared to the pharmacophore features shown in Figure 4a, the directional character of the H attached to a cationic N is absent in Figure 4b, even though in principle the H attached to a quaternary N is oriented in one direction only. The lack of directional feature in this case was probably due to the pharmacophore generation process itself (the methodological part). In addition, our current proposed model bears certain resemblance to earlier models.<sup>15,17a</sup>

The factors responsible for the D3 preference for most of these compounds ((+)-**6**, (–)-**7**, and **1**) cannot be addressed by the present pharmacophore completely. In our opinion, the highest selectivity for D3 exhibited by (–)-**11** may be due to the presence of an additional aryl ring extending beyond those present in rest of the molecules. Also, as seen from the representative top scoring hypotheses (gauche and anti conformations of the ethylene linker), we strongly believe that the conformation of this linker is critical for interaction with either or both D2/D3 receptors. In addition, at this point in time, no information is available regarding the role of either or both



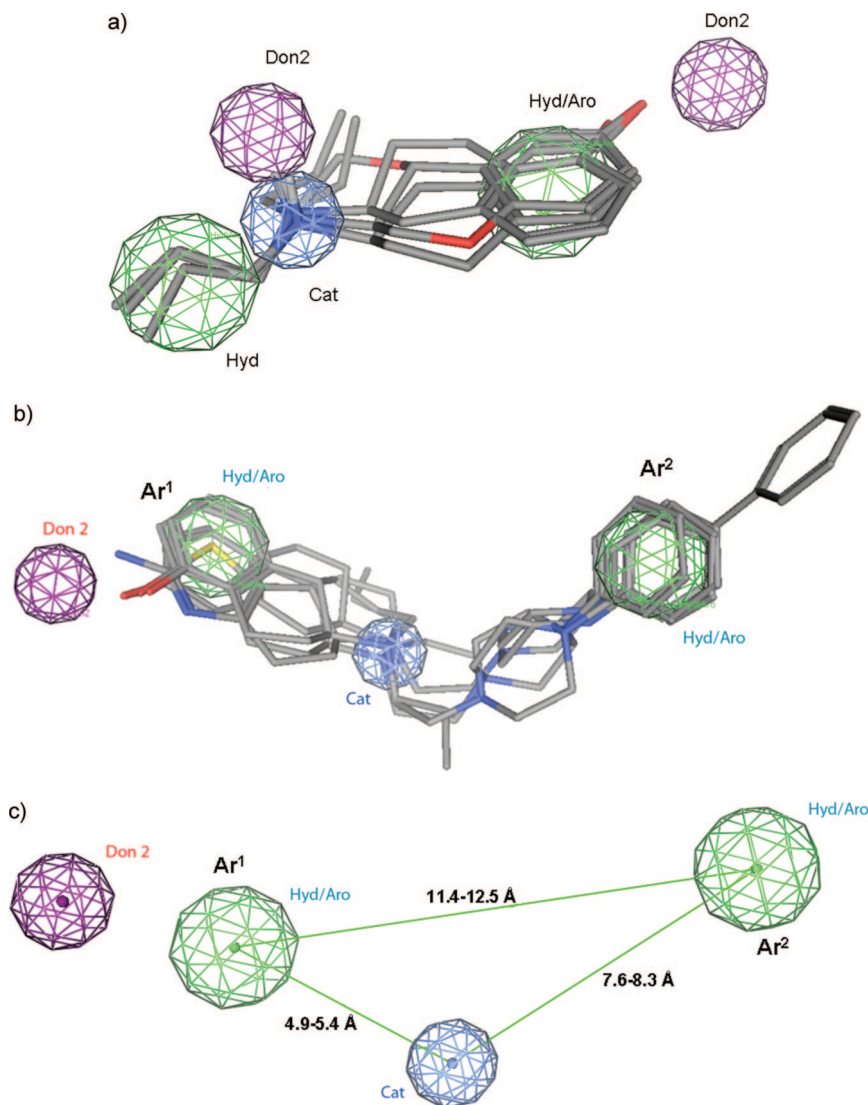


**Figure 4.** (a) Three-point pharmacophore generated using known D2/D3 ligands, (b) three-point pharmacophore derived from D2/D3 ligand hybrid analogues, and (c) three-point pharmacophore derived from hybrid analogues with corresponding interfeature distances: Aro/Hyd, Aromatic/Hydrophobic; cat., cationic; Don2, the directional feature toward which the H-bond donor should be oriented. Ar<sup>1</sup> denotes the aromatic ring of either aminotetralin or 2-aminothiazole moieties, and Ar<sup>2</sup> is the phenyl ring attached to one of the piperazine nitrogens.

**Table 2.** Pharmacophoric Distances for the Gauche and Anti-Conformations of the Hybrid Analogues

compd	interfeature distance (Å) <sup>a</sup>					
	gauche <sup>b</sup>			anti <sup>b</sup>		
	N <sup>+</sup> –Ar <sup>1</sup>	N <sup>+</sup> –Ar <sup>2</sup>	Ar <sup>1</sup> –Ar <sup>2</sup>	N <sup>+</sup> –Ar <sup>1</sup>	N <sup>+</sup> –Ar <sup>2</sup>	Ar <sup>1</sup> –Ar <sup>2</sup>
(+)- <b>6</b>	5.06	8.50	12.26	5.00	8.73	12.95
(–)- <b>6</b>	5.14	8.57	12.62	5.13	9.26	13.66
<b>11</b>	4.92	8.51	12.00	4.89	8.59	12.24
(–)- <b>8</b>	5.13	8.52	12.66	5.15	9.26	13.72

<sup>a</sup> N<sup>+</sup> represents the cationic feature. Ar<sup>1</sup> denotes the aromatic ring of either aminotetralin or 2-aminothiazole moieties, and Ar<sup>2</sup> is the phenyl ring attached to one of the piperazine nitrogens. The distance N<sup>+</sup>–Ar<sup>1</sup> is the distance between the cationic N and the ring centroid of Ar<sup>1</sup>. <sup>b</sup> The terms gauche and anti represent the conformation of the ethylene bridge connecting cationic N with the arylpiperazine moiety.

piperazine N-atom(s) on affinity and selectivity. Our future efforts will be focused on addressing these critical questions and further refining this pharmacophore model. The hybrid analogue concept representing D2/D3 receptor interaction requirements could possibly address otherwise difficult to explore selectivity requirements. In addition to further enhancing our understanding of D2/D3 ligand structural requirements

pertaining to selectivity, it may shed light on requirements for potency and aid in the design of potent and selective D2/D3 ligands/agonists. Certainly, the arylpiperazine portion of the hybrid structures has a vital, yet complex, role to play in imparting the higher potency compared to nonhybrid DA ligands and also potentially plays a role in endowing selectivity for one receptor over the other. Efforts are underway to identify molecular determinants for potency and selectivity of these hybrid structures, and our forthcoming publications will attempt to address this with the help of carefully designed structures. This will further help us to refine the preliminary pharmacophore proposed in this article.

## Conclusion

In this manuscript we have carried out further modifications of our hybrid derivatives by converting them into structurally constrained versions to understand their mode of interaction in general with DA D2 and D3 receptors and also to obtain an insight into bioactive conformational structures of these molecules. For this purpose, several 1,2,3,4,4a,5,10,10a-octahydrobenz[g]quinoline-ol and 1,2,3,4,4a-5,6,10b-octahydrobenzo[f]quinolin-ol based hybrid derivatives were prepared and biologically characterized. In this



regard, as pointed out earlier, octahydrobenzo[*f* and *g*]quinolinol related derivatives as constrained molecules of aminotetralin structures (7-OH-DPAT and 5-OH-DPAT) were synthesized before for interaction with DA receptors. However, none of those derivatives were evaluated in detailed binding interaction with D2 and D3 receptors, as they were mainly characterized in functional assays and in some cases in binding assay for the D2 receptor. Therefore, precise information on binding interactions with D2/D3 receptors was not available. The present results from constrained hybrids indicate that a compound with structure 1,2,3,4,4a,5,6,10b-octahydrobenzo[*f*]quinolinol, e.g., (–)-**8**, exhibits high affinity for D2/D3 receptors and in this regard is significantly more potent than the corresponding nonhybrid version. Similar results were found with other lead compounds when compared with the corresponding nonhybrid version. Our study with the hybrid version of these constrained derivatives as well as other lead hybrid compounds provides some unique information about the interaction of these compounds with DA receptors. These results clearly indicate a significant contribution of the piperazine moiety in enhancing interaction of hybrid derivatives with DA receptor subtypes. Our results prompt the proposal of a unique pharmacophore structure for hybrid derivatives consisting of three pharmacophoric centers. This unique pharmacophore structure will be further refined by incorporating the results of future studies.

## Experimental Section

Analytical silica gel-coated TLC plates (silica gel 60 F<sub>254</sub>) were purchased from EMD Chemical, Inc., and were visualized with UV light by treatment with phosphomolybdic acid (PMA), Dragendorff's reagent, or ninhydrin. Flash column chromatography was carried out on Whatman Purasil 60A silica gel 230–400 mesh. <sup>1</sup>H NMR spectra were routinely obtained on Varian 400 MHz FT NMR equipment. The NMR solvent used was CDCl<sub>3</sub>, CD<sub>3</sub>OD, or DMSO-*d*<sub>6</sub> as indicated. TMS was used as an internal standard. Elemental analysis was performed by Atlantic Microlab, Inc., and were within ±0.4% of the theoretical value. Optical rotations were recorded on Perkin-Elmer 241 polarimeter.

**Procedure A. 2-Chloro-1-(4-phenylpiperazin-1-yl)ethanone (13a).** 1-Phenylpiperazine **12a** (3 g, 18.5 mmol) and triethylamine (3.34 mL, 22.2 mmol) were dissolved in 100 mL of CH<sub>2</sub>Cl<sub>2</sub> and cooled to 0 °C. Chloroacetyl chloride (1.9 mL, 22.2 mmol) was added slowly over the course of 5 min. The mixture was allowed to stir at 0 °C for 30 min, at which time saturated NaHCO<sub>3</sub> (100 mL) was added. The organic layer was separated, dried (Na<sub>2</sub>SO<sub>4</sub>), filtered, and concentrated. The crude solid was then recrystallized from EtOAc to give 4.3 g (97%) of 2-chloro-1-(4-phenylpiperazin-1-yl)ethanone **13a**. <sup>1</sup>H NMR (400 MHz, CDCl<sub>3</sub>) δ 3.47 (bs, 4H), 3.59 (bs, 4H), 4.25 (s, 2H), 6.53–6.55 (d, 1H, *J* = 7.6 Hz), 6.64–6.66 (d, 1H, *J* = 7.6 Hz), 6.83–6.87 (t, 1H, *J* = 8 Hz).

**2-Chloro-1-[4-(2,3-dichlorophenyl)piperazin-1-yl]ethanone (13b).** This compound was prepared following procedure A using 2 g (7.47 mmol) of 1-(2,3-dichlorophenyl)piperazine, 0.92 mL (8.22 mmol) of chloroacetyl chloride, and 2 mL (15 mmol) of triethylamine to give 2.6 g (87%) of **13b** as a solid. <sup>1</sup>H NMR (400 MHz, CDCl<sub>3</sub>) δ 3.43 (bs, 4H), 4.27 (s, 2H), 3.61 (bs, 4H), 6.41–4.49 (m, 2H), 6.90–6.93 (t, 1H, *J* = 8 Hz).

**4-Chloro-1-(4-phenylpiperazin-1-yl)butan-1-one (13c).** This compound was prepared following procedure A using 2 g (12.3 mmol) of 1-phenylpiperazine, 1.91 g (13.6 mmol) of 4-chlorobutanoyl chloride, and 2 mL (15 mmol) of triethylamine to give 3.19 g (97%) of solid **13c**. <sup>1</sup>H NMR (400 MHz, CDCl<sub>3</sub>) δ 1.94–1.98 (m, 2H), 2.32–2.34 (t, 2H, *J* = 8 Hz), 3.33–3.35 (m, 4H), 3.48–3.50 (m, 4H), 3.67–3.67 (t, 2H, *J* = 8 Hz), 6.53–6.55 (d, 1H, *J* = 7.6 Hz), 6.64–6.66 (d, 1H, *J* = 7.6 Hz), 6.83–6.87 (t, 1H, *J* = 8 Hz).

**2-(3-Methoxybenzyl)nicotinic Acid Methyl Ester (16).** Activated zinc dust (1.75 g, 27.3 mmol) was added to 20 mL of dry THF and the suspension cooled to 0 °C. 3-Methoxybenzyl bromide **14** (1.90 mL, 13.6 mmol) was added, and this mixture was stirred

at 0 °C under a N<sub>2</sub> atmosphere for 2 h. Stirring was stopped, and the excess zinc was allowed to settle. The benzylzinc bromide was then added via cannulation to a suspension of bis(triphenylphosphine)nickel(II) chloride (1.78 g, 27.3 mmol) and methyl 2-chloronicotinate (1.17 g, 6.82 mmol) in 100 mL of dry THF. This mixture was stirred at ambient temperature for 48 h. The reaction was quenched by the addition of 10% NH<sub>4</sub>Cl (100 mL), and the product was extracted with ethyl acetate, dried (Na<sub>2</sub>SO<sub>4</sub>), filtered, and concentrated. The crude mixture was dissolved in ether, and ethereal HCl was added. The salt was recovered by filtration and used without further purification to yield 1.57 g of **16** (free base, 90%). <sup>1</sup>H NMR (400 MHz, CDCl<sub>3</sub>) δ 3.75 (s, 3H), 3.87 (s, 3H), 4.56 (s, 2H), 6.70–6.73 (m, 1H), 6.81–6.85 (m, 1H), 7.15–7.19 (t, 1H, *J* = 8 Hz), 7.22–7.26 (m, 2H), 8.16–8.18 (dd, 1H, *J* = 1.6 Hz, *J* = 8 Hz), 8.68–8.7 (dd, 1H, *J* = 1.6 Hz, *J* = 8 Hz).

**cis- and trans-2-(3-Methoxybenzyl)piperidine-3-carboxylic Acid Methyl Ester (17).** The hydrochloride salt of pyridine **16** (5.75 g, 19.2 mmol) was dissolved in 200 mL of MeOH, and 200 mg of PtO<sub>2</sub> was added. The mixture was then hydrogenated at 45 psi for 24 h. The mixture was filtered through a pad of Celite and the solvent removed in vacuo to yield a mixture of *cis*- and *trans*-amine **17** isomers as an oil (4.77 g, 95%), which were used without further purification and were not separated in the subsequent transformations. <sup>1</sup>H NMR (CDCl<sub>3</sub>) δ 7.18–7.25 (t, 1H, *J* = 8 Hz), 6.72–6.79 (m, 3H), 3.80 (s, 3H), 3.72 (s, 3H), 3.0–3.12 (m, 2H), 2.84–2.9 (m, 1H), 2.57–2.77 (m, 3H), 1.8–2.2 (m, 1H), 1.76–1.82 (m, 2H), 1.66–1.73 (m, 2H), 1.42–1.46 (m, 1H).

**cis- and trans-2-(3-Methoxybenzyl)piperidine-1,3-dicarboxylic Acid Dimethyl Ester (18).** Amine **17** (1.58 g, 6.03 mmol) was added to a suspension of 1.9 g (13 mmol) of K<sub>2</sub>CO<sub>3</sub> in 20 mL of dichloromethane. Methyl chloroformate (0.93 mL, 12 mmol) was added, and the mixture was stirred for 3 h at ambient temperature. Water (20 mL) was added and the product was extracted with CH<sub>2</sub>Cl<sub>2</sub>, dried (Na<sub>2</sub>SO<sub>4</sub>), filtered, and concentrated to yield the crude carbamate **18** as an oil (1.9 g, 100%), which was used without further purification. <sup>1</sup>H NMR (400 MHz, CDCl<sub>3</sub>) δ 1.66–2.0 (m, 3H), 2.50–2.54 (m, 1H), 2.64–2.77 (m, 2H), 2.87–2.99 (m, 2H), 3.33 (m, 2H), 3.58–3.60 (m, 2H), 3.69 (s, 3H), 3.80 (s, 3H), 4.8–4.98 (m, 1H), 4.1–4.16 (m, 1H), 6.62–6.80 (m, 3H), 7.15–1.18 (t, 1H, *J* = 8 Hz).

**(±)-cis-8-Methoxy-5-oxo-3,4,4a,5,10,10a-hexahydro-2H-benzo[*g*]quinoline-1-carboxylic Acid Methyl Ester (19).** Methyl ester **18** (910 mg, 2.83 mmol) was dissolved in 30 mL of MeOH. LiOH (102 mg, 4.25 mmol) and water (7 mL) were added, and the mixture was allowed to stir at room temperature for 24 h. Methanol was then evaporated, and the mixture was partitioned between water and ethyl acetate. The aqueous phase was then acidified and extracted with several portions of ethyl acetate. The combined organic fractions were dried (Na<sub>2</sub>SO<sub>4</sub>), filtered, and concentrated to yield the crude acid, which was used without further purification. Then 800 mg (2.6 mmol) of the acid was dissolved in 30 mL of dichloromethane. SOCl<sub>2</sub> (0.23 mL, 13.4 mmol) was added, and the mixture was refluxed until no more HCl gas was produced. The mixture was cooled and concentrated to yield the crude acid chloride, which was dissolved in 40 mL of dry CH<sub>2</sub>Cl<sub>2</sub> and cooled to 0 °C. TiCl<sub>4</sub> (1 M in CH<sub>2</sub>Cl<sub>2</sub>, 5.2 mL, 5.2 mmol) was added dropwise, and this mixture was stirred in an ice bath for 2 h. The reaction was quenched by the addition of saturated NaCl (20 mL), and the product was extracted with CH<sub>2</sub>Cl<sub>2</sub>. The organic layer was dried (Na<sub>2</sub>SO<sub>4</sub>), filtered, and concentrated. The product was purified by column chromatography (94:5:1 EtOAc/MeOH/Et<sub>3</sub>N) to yield only the *cis*-isomer **19** as a yellow solid (480 mg, 63%). <sup>1</sup>H NMR (400 MHz, CDCl<sub>3</sub>) δ 1.59–1.62 (m, 1H), 1.78–1.82 (m, 1H), 1.91–1.97 (m, 1H), 2.69–2.72 (m, 1H), 2.72–2.82 (m, 1H), 2.92–3.1 (m, 1H), 3.3–3.4 (m, 1H), 3.72 (s, 3H), 3.89 (s, 3H), 4.1–4.18 (m, 1H), 4.79–4.81 (m, 1H), 6.65–6.67 (m, 1H), 6.83–6.87 (m, 1H), 8.01–8.04 (d, 1H, *J* = 8 Hz).

**(±)-cis-8-Methoxy-3,4,4a,5,10,10a-hexahydro-2H-benzo[*g*]quinoline-1-carboxylic Acid Methyl Ester (20).** Ketone (±)-**19** (610 mg, 2.1 mmol) and 1.5 mL of 70% perchloric acid were dissolved in 25 mL of acetic acid. Then 60 mg of Pd/C was then



added and the mixture was hydrogenated at 45 psi for 34 h. The catalyst was filtered through a pad of Celite, and acetic acid was evaporated. The residue was washed with 20% NaOH, dried ( $\text{Na}_2\text{SO}_4$ ), filtered, and concentrated to yield 510 mg (88%) of **20** as an oil, which was used without further purification.  $^1\text{H}$  NMR (400 MHz,  $\text{CDCl}_3$ )  $\delta$  1.40–1.6 (m, 3H), 1.6–1.71 (m, 1H), 2.03–2.07 (m, 1H), 2.55–2.59 (d, 1H,  $J = 8$  Hz), 2.85–3.1 (m, 3H), 2.71–2.82, 3.71 (m, 3H), 3.76 (m, 3H), 4.16–4.21 (m, 1H), 4.45–4.51 (m, 1H), 6.59–6.6 (m, 1H), 6.68–6.71 (m, 1H), 6.96–6.98 (d, 2H,  $J = 8$  Hz).

( $\pm$ )-**cis-8-Methoxy-1,2,3,4,4a,5,10,10a-octahydrobenzo[g]-quinoline (21)**. Carbamate **20** (350 mg, 1.27 mmol) was added to a solution of KOH (240 mg, 7.64 mmol), water (0.13 mL, 7.64 mmol), and hydrazine hydrate (0.24 mL, 7.64 mmol) in ethylene glycol (20 mL). This mixture was refluxed for 3 h, at which time the solution was cooled and poured into water and the product was extracted with several portions of ethyl acetate. After the mixture was dried, filtered, and concentrated, 182 mg (90%) of the titled product **21** was recovered as a sticky oil.  $^1\text{H}$  NMR (400 MHz,  $\text{CDCl}_3$ )  $\delta$  1.38–1.43 (m, 1H), 1.55 (s, 1H), 1.66–1.74 (m, 3H), 1.96–2.2 (m, 1H), 2.5–2.75 (m, 3H), 2.92–3.10 (m, 4H), 3.72 (s, 3H), 6.55–6.2 (m, 1H), 6.68–6.67 (m, 1H), 6.96–7.00 (d, 2H,  $J = 8$  Hz).

**Procedure B.** ( $\pm$ )-**cis-2-(8-Methoxy-3,4,4a,5,10,10a-hexahydro-2-H-benzo[g]quinolin-1-yl)-1-(4-phenylpiperazin-1-yl)ethanone (22a)**. A mixture of amine ( $\pm$ )-**21** (390 mg, 1.8 mmol), chloride **13a** (514 mg, 2.16 mmol), and  $\text{K}_2\text{CO}_3$  (745 mg, 5.4 mmol) in acetonitrile (40 mL) was heated at reflux for 1 h. The mixture was then cooled, filtered, and concentrated. The product was purified by column chromatography using ethyl acetate as an eluent to yield **22a** (460 mg, 61%) as a solid.  $^1\text{H}$  NMR (400 MHz,  $\text{CDCl}_3$ )  $\delta$  1.5–1.6 (m, 4H), 1.72–1.8 (m, 1H), 2.9–3.1 (m, 4H), 2.7–2.82 (m, 7H), 3.2–3.29 (m, 1H), 3.38–3.5 (m, 2H), 3.54–3.58 (m, 1H), 3.78 (s, 3H), 7.25–7.30 (m, 2H), 6.62–6.64 (m, 1H), 6.68–6.7 (m, 1H), 6.84–6.9 (m, 3H), 6.96–7.0 (d, 1H,  $J = 8$  Hz).

( $\pm$ )-**cis-1-[4-(2,3-Dichlorophenyl)piperazin-1-yl]-2-(8-methoxy-3,4,4a,5,10,10a-hexahydro-2H-benzo[g]quinolin-1-yl)ethanone (22b)**. Amine ( $\pm$ )-**21** (200 mg, 0.8 mmol), chloride **13b** (290 mg, 0.95 mmol), and  $\text{K}_2\text{CO}_3$  (328 mg, 2.4 mmol) were reacted according to procedure B. The product was purified by column chromatography using ethyl acetate as an eluent to yield 354 mg (92%) of **22b** as a solid.  $^1\text{H}$  NMR (400 MHz,  $\text{CDCl}_3$ )  $\delta$  1.50–1.61 (m, 3H), 1.76–1.83 (m, 1H), 2.14 (bs, 1H), 2.3–2.4 (m, 1H), 2.52–2.8 (m, 10H), 3.01–3.07 (m, 2H), 3.32–3.40 (m, 2H), 3.51–3.56 (m, 2H), 3.75 (s, 3H), 6.61–6.62 (m, 1H), 6.65–6.68 (m, 1H), 6.82–6.86 (m, 1H), 6.94–6.96 (dd, 1H,  $J = 1.8$  Hz,  $J = 8$  Hz), 7.13–7.19 (m, 2H).

**Procedure C.** ( $\pm$ )-**cis-1-[2-(4-Phenylpiperazin-1-yl)ethyl]-1,2,3,4,4a,5,10,10a-octahydrobenzo[g]quinolin-8-ol (23a)**. Lithium aluminum hydride (244 mg, 6.44 mmol) was added to dry THF (50 mL), and the suspension was cooled to 0 °C. A solution of amide **22a** (450 mg, 1.0 mmol) in THF (15 mL) was added dropwise, and the mixture was refluxed for 3 h. The mixture was cooled in an ice bath and quenched with 10% NaOH, and the resulting solids were filtered. The filtrate was dried ( $\text{Na}_2\text{SO}_4$ ), filtered, and concentrated to yield amine **23a** (235 mg, 98%) as an oil, which was used without further purification.  $^1\text{H}$  NMR (400 MHz,  $\text{CDCl}_3$ )  $\delta$  1.51–1.62 (m, 4H), 1.70–1.81 (m, 1H), 2.92–3.11 (m, 4H), 2.72–2.86 (m, 9H), 3.22–3.30 (m, 1H), 3.37–3.50 (m, 2H), 3.55–3.58 (m, 1H), 3.77 (s, 3H), 7.24–7.29 (m, 2H), 6.63–6.65 (m, 1H), 6.67–6.7 (m, 1H), 6.85–6.9 (m, 3H), 6.97–7.01 (d, 1H,  $J = 8$  Hz).

( $\pm$ )-**cis-1-[4-(2,3-Dichloro-phenyl)piperazin-1-yl]-2-(8-methoxy-3,4,4a,5,10,10a-hexahydro-2H-benzo[g]quinolin-1-yl)ethanone (23b)**. Compound **22b** (354 mg, 0.725 mmol) was reduced following procedure C to yield 338 mg (98%) of **23b** as an oil.  $^1\text{H}$  NMR (400 MHz,  $\text{CDCl}_3$ )  $\delta$  1.51–1.60 (m, 3H), 1.75–1.82 (m, 1H), 2.15 (bs, 1H), 2.31–2.4 (m, 1H), 2.50–2.87 (m, 12H), 3.010–3.05 (m, 2H), 3.30–3.39 (m, 2H), 3.52–3.55 (m, 2H), 3.78

(s, 3H), 6.60–6.62 (m, 1H), 6.66–6.69 (m, 1H), 6.83–6.87 (m, 1H), 6.95–6.97 (dd, 1H,  $J = 1.8$  Hz,  $J = 8$  Hz), 7.14–7.20 (m, 2H).

**Procedure D.** **cis-1-[2-(4-Phenylpiperazin-1-yl)ethyl]-1,2,3,4,4a,5,10,10a-octahydrobenzo[g]quinolin-8-ol (24a)**. Compound ( $\pm$ )-**23a** (310 mg, 0.76 mmol) was dissolved in 40 mL of dichloromethane and cooled to  $-78$  °C. Then 1.5 mL of  $\text{BBr}_3$  (1 M in  $\text{CH}_2\text{Cl}_2$ ) was added dropwise and the mixture was allowed to warm to ambient temperature and stirred overnight. Saturated  $\text{NaHCO}_3$  (50 mL) was added, and the product was extracted with  $\text{CH}_2\text{Cl}_2$ . The organic extracts were dried ( $\text{Na}_2\text{SO}_4$ ), filtered, and concentrated. The titled compound was then purified by column chromatography using 94:5:1 EtOAc/MeOH/Et<sub>3</sub>N to yield ( $\pm$ )-**24a** (233 mg, 78%) as a tan solid.  $^1\text{H}$  NMR (400 MHz,  $\text{CDCl}_3$ )  $\delta$  1.35–1.43 (m, 2H), 1.6–1.77 (m, 2H), 2.1–2.19 (m, 1H), 2.55–2.84 (m, 14H), 2.92–3.0 (m, 1H), 3.09–3.2 (m, 1H), 3.18–3.22 (m, 4H), 6.36–6.38 (m, 1H), 6.52–6.55 (m, 1H), 6.82–6.91 (m, 4H), 7.22–7.28 (m, 2H). The free base was converted to its HCl salt, mp =  $174$ – $177$  °C. Anal. ( $\text{C}_{25}\text{H}_{33}\text{N}_3\text{O} \cdot 2\text{HCl}$ ) C, H, N.

( $\pm$ )-**cis-1-[2-[4-(2,3-Dichlorophenyl)piperazin-1-yl]ethyl]-1,2,3,4,4a,5,10,10a-octahydrobenzo[g]quinolin-8-ol (24b)**. Compound **22b** (338 mg, 0.714 mmol) was demethylated following procedure D, giving ( $\pm$ )-**24b**, 267 mg (80%), as a tan solid.  $^1\text{H}$  NMR (400 MHz,  $\text{CDCl}_3$ )  $\delta$  1.35–1.43 (m, 2H), 1.6–1.77 (m, 2H), 2.1–2.19 (m, 1H), 2.55–2.84 (m, 14H), 2.92–3.0 (m, 1H), 3.09–3.2 (m, 1H), 3.18–3.22 (m, 4H), 6.36–6.38 (m, 1H), 6.52–6.55 (m, 1H), 6.82–6.91 (m, 4H), 7.22–7.28 (m, 2H). The free base was then converted to its HCl salt, mp =  $161$ – $165$  °C. Anal. ( $\text{C}_{25}\text{H}_{31}\text{Cl}_2\text{N}_3\text{O} \cdot 2\text{HCl}$ ) C, H, N.

**2-Hydroxy-7-methoxy-3,4-dihydronaphthalene-1-carboxylic Acid Methyl Ester (26)**. 7-Methoxy-2-tetralone **25** (12.5 g, 76 mmol) and NaH (5.6 g, 0.145 mol) were refluxed in benzene (200 mL) for 30 min, at which time dimethyl carbonate (12 mL, 0.145 mol) was added and refluxing was continued for 3 h. The mixture was cooled and then carefully quenched by the addition of water (50 mL), and the product was extracted with ethyl acetate, dried ( $\text{Na}_2\text{SO}_4$ ), filtered, and concentrated to yield the product, which was purified by column chromatography (1:1 hexane/EtOAc) to give 16 g of **26** (96%) as a liquid.  $^1\text{H}$  NMR (400 MHz,  $\text{CDCl}_3$ )  $\delta$  2.50–2.54 (t, 2H,  $J = 8$  Hz), 2.73–2.77 (t, 2H,  $J = 8$  Hz), 3.8 (s, 3H), 3.92 (s, 3H), 6.60–6.63 (dd, 1H,  $J = 2$  Hz, 8 Hz), 7.02–7.05 (d, 1H,  $J = 8$  Hz), 7.30–7.31 (d, 2H,  $J = 2$  Hz), 13.38 (s, 1H).

**3-(2-Cyanoethyl)-2-hydroxy-7-methoxy-3,4-dihydronaphthalene-1-carboxylic Acid Methyl Ester (27)**. *n*-Butyllithium (55.6 mL, 0.138 mol) was added to a solution of diisopropylamine (19.3 mL, 0.138 mol) in dry THF (100 mL) at  $-78$  °C and stirred for 15 min, then warmed to 0 °C and stirred for an additional 15 min. Next, a solution of **26** (12.9 g, 0.055 mol) dissolved in THF (20 mL) was added slowly and the mixture was stirred at 0 °C for 1 h. Chloropropionitrile (5.6 mL, 0.071 mol) was then added, and this solution was stirred at room temperature for 1 h and carefully quenched with 50 mL of 1 M HCl. The product was extracted with ethyl acetate (3  $\times$  50 mL), dried ( $\text{Na}_2\text{SO}_4$ ), filtered, and concentrated. The crude oil was then purified by column chromatography (1:1 hexane/EtOAc) to yield **27**, 7.28 g (46%), as an oil.  $^1\text{H}$  NMR (400 MHz,  $\text{CDCl}_3$ )  $\delta$  1.70–1.76 (m, 1H), 1.88–1.94 (m, 1H), 2.41–2.50 (m, 2H), 2.57–2.67 (m, 1H), 2.82–2.86 (t, 1H,  $J = 6.8$  Hz), 2.97–3.01 (m, 1H), 3.80 (s, 3H), 3.93 (s, 3H), 13.4 (s, 1H), 6.63–6.65 (dd, 1H,  $J = 2$  Hz,  $J = 8$  Hz), 7.03–7.05 (d, 1H,  $J = 8$  Hz), 7.30–7.31 (d, 1H,  $J = 8$  Hz).

**3-(6-Methoxy-3-oxo-1,2,3,4-tetrahydronaphthalen-2-yl)propionitrile (28)**. Methyl ester **27** (430 mg, 1.5 mmol), LiCl (63 mg, 1.5 mmol), water (2 mL), and DMSO (1 mL) were refluxed for 4 h. The solution was then cooled and poured into water (15 mL) and the product extracted with several portions of ethyl acetate (3  $\times$  15 mL). The organic extracts were pooled, dried ( $\text{Na}_2\text{SO}_4$ ), filtered, and concentrated to yield 243 mg (71%) of **28** as an oil, which was used directly in the next step.  $^1\text{H}$  NMR (400 MHz,  $\text{CDCl}_3$ )  $\delta$  1.63–1.79 (m, 1H), 2.16–2.21 (m, 1H), 2.54–2.56 (m, 2H), 2.62–2.67 (m, 1H), 2.76–2.88 (m, 1H), 3.05–3.10 (dd, 1H,



$J = 5.6$  Hz,  $J = 8$  Hz), 3.55–3.70 (q, 2H,  $J = 6$  Hz), 6.65–6.66 (m, 1H), 3.80 (s, 3H), 6.76–6.79 (dd, 1H,  $J = 2.4$  Hz,  $J = 8$  Hz), 7.11–7.13 (d, 1H,  $J = 8$  Hz).

**3-(7'-Methoxy-3',4'-dihydro-1'H-spiro[[1,3]dioxolane-2,2'-naphthalen]-3'-yl)propionitrile (29).** A solution of ketone **28** (280 mg, 1.22 mmol), triethyl orthoformate (0.71 mL, 4.3 mmol), ethylene glycol (1.2 mL), and TsOH (5 mg, 0.012 mmol) in dichloromethane (20 mL) was stirred overnight at room temperature. The reaction mixture was then poured into water (30 mL) and the organic layer was separated, dried ( $\text{Na}_2\text{SO}_4$ ), filtered, and concentrated to yield an oil which was purified by column chromatography (EtOAc) to yield **29** 332 mg (98%).  $^1\text{H}$  NMR (400 MHz,  $\text{CDCl}_3$ )  $\delta$  1.50–1.62 (m, 1H), 2.01–2.19 (m, 2H), 2.40–2.59 (m, 2H), 2.65–2.71 (m, 1H), 2.82–3.32 (m, 2H), 3.76 (m, 3H), 3.80–4.09 (m, 4H), 6.56–6.57 (m, 1H), 6.70–6.72 (dd, 1H,  $J = 2.8$  Hz,  $J = 8$  Hz), 7.00–7.03 (d, 1H,  $J = 8$  Hz).

**3-(7'-Methoxy-3',4'-dihydro-1'H-spiro[[1,3]dioxolane-2,2'-naphthalen]-3'-yl)propylamine (30).** Nitrile **29** (350 mg, 1.28 mmol) was dissolved in 30 mL of MeOH. Raney nickel (200 mg) was added, and the mixture was hydrogenated overnight. The reaction solution was filtered through a pad of Celite and concentrated to give 300 mg of **30** (62%) as a solid which was used without further purification.  $^1\text{H}$  NMR (400 MHz,  $\text{CDCl}_3$ )  $\delta$  1.10–1.79 (m, 6H), 1.92–2.0 (m, 1H), 2.60–3.16 (m, 6H), 3.67–3.79 (m, 3H), 3.82–4.10 (m, 4H), 6.56–6.57 (m, 1H), 6.70–6.72 (dd, 1H,  $J = 2.8$  Hz,  $J = 8$  Hz), 7.01–7.04 (d, 1H,  $J = 8$  Hz).

**( $\pm$ )-trans-8-Methoxy-1,2,3,4,4a,5,10,10a-octahydrobenzo[g]-quinoline (32).** Amine **30** (300 mg, 1.1 mmol) was dissolved in 20 mL of MeOH, and 5 mL of 6 M HCl was added. The solution was refluxed for 2 h, cooled, and concentrated to yield the iminium salt intermediate **31**. The crude solid was then dissolved in 40 mL of MeOH.  $\text{NaCNBH}_3$  (65 mg, 1.02 mmol) was added and the solution stirred for 1 h at ambient temperature. Methanol was then evaporated, and the residue was partitioned between saturated  $\text{NaHCO}_3$  (50 mL) and ethyl acetate (50 mL). The organic layer was separated, dried ( $\text{Na}_2\text{SO}_4$ ), filtered, and concentrated. The crude amine was then purified by column chromatography (95:4:1 EtOAc/MeOH/ $\text{Et}_3\text{N}$ ) to give **32**, 187 mg (80%), in solid form.  $^1\text{H}$  NMR (400 MHz,  $\text{CDCl}_3$ )  $\delta$  1.11–1.26 (m, 1H), 1.46–1.73 (m, 4H), 1.91–1.95 (m, 1H), 2.37–2.43 (m, 1H), 2.57–2.76 (m, 4H), 2.83–2.88 (m, 1H), 3.10–3.14 (m, 1H), 3.77 (s, 3H), 6.61–6.62 (m, 1H), 6.67–6.97 (dd, 1H,  $J = 2.8$  Hz,  $J = 8$  Hz), 6.96–6.98 (d, 1H,  $J = 8$  Hz).

**( $\pm$ )-trans-2-(8-Methoxy-3,4,4a,5,10,10a-hexahydro-2H-benzo[g]quinolin-1-yl)-1-(4-phenylpiperazin-1-yl)ethanone (33a).** Amine **32** (110 mg, 0.5 mmol), chloride **13a** (202 mg, 0.66 mg), and  $\text{K}_2\text{CO}_3$  (175 mg, 1.27 mmol) were refluxed following procedure B. The crude solid **33a** (190 mg) was used without further purification.  $^1\text{H}$  NMR (400 MHz,  $\text{CDCl}_3$ )  $\delta$  1.50–1.20 (m, 1H), 1.6–1.7 (m, 1H), 1.84–1.90 (m, 1H), 2.30–2.48 (m, 3H), 2.17 (s, H), 2.62–2.79 (m, 1H), 2.50–3.1 (m, 5H), 3.5–3.36 (m, 2H), 3.53–3.62 (m, 1H), 3.68–3.74 (m, 1H), 3.79 (s, 3H), 3.95–4.17 (m, 1H), 3.99–4.13 (m, 1H), 6.62–6.70 (m, 2H), 6.89–6.97 (m, 4H), 7.26–7.31 (m, 2H).

**( $\pm$ )-trans-1-[4-(2,3-Dichlorophenyl)piperazin-1-yl]-2-(8-methoxy-3,4,4a,5,10,10a-hexahydro-2H-benzo[g]quinolin-1-yl)ethanone (33b).** Amine **32** (70 mg, 0.277 mmol) and chloride **13b** (93 mg, 0.30 mmol) were treated with  $\text{K}_2\text{CO}_3$  (76 mg, 0.55 mmol) following procedure B to yield 126 mg of crude solid **33b**, which was used without further purification.  $^1\text{H}$  NMR  $\delta$  (400 MHz,  $\text{CDCl}_3$ ) 1.50–1.20 (m, 1H), 1.6–1.7 (m, 1H), 1.84–1.90 (m, 1H), 2.17 (s, H), 2.30–2.48 (m, 3H), 2.62–2.79 (m, 1H), 2.80–3.1 (m, 5H), 3.5–3.36 (m, 2H), 3.53–3.62 (m, 1H), 3.68–3.74 (m, 1H), 3.79 (s, 3H), 3.95–4.10 (m, 1H), 4.12–4.14 (m, 1H), 6.62–6.70 (m, 2H), 6.89–6.97 (m, 4H), 7.26–7.31 (m, 2H).

**( $\pm$ )-trans-(8-Methoxy-3,4,4a,5,10,10a-hexahydro-2H-benzo[g]quinolin-1-yl)-1-(4-phenylpiperazin-1-yl)butan-1-one (33c).** This compound was prepared using 200 mg of amine **32** (0.79 mmol), 288 mg of chloride **13c** (0.945 mmol), and 327 mg of  $\text{K}_2\text{CO}_3$  (2.37 mmol) according to procedure B. Column chromatography using EtOAc as eluent afforded **33c** 330 mg (93%).  $^1\text{H}$  NMR (400 MHz,

$\text{CDCl}_3$ )  $\delta$  1.20–1.34 (m, 1H), 1.79–1.81 (m, 1H), 1.91–2.23 (m, 5H), 2.41–2.50 (m, 5H), 2.79–2.82 (m, 1H), 3.0–3.41 (m, 9H), 3.62–3.80 (m, 7H), 6.60–6.63 (m, 1H), 6.68–6.72 (m, 1H), 6.89–6.95 (m, 4H), 7.26–7.31 (m, 2H).

**( $\pm$ )-trans-8-Methoxy-1-[2-(4-phenylpiperazin-1-yl)ethyl]-1,2,3,4,4a,5,10,10a-octahydrobenzo[g]quinoline (34a).** Amide **33a** (110 mg, 0.262 mmol) was reduced with lithium aluminum hydride (70 mg, 1.31 mmol) following procedure C to yield 105 mg of solid **34a** in 99% yield.  $^1\text{H}$  NMR (400 MHz,  $\text{CDCl}_3$ )  $\delta$  1.13–1.23 (m, 1H), 1.61–1.76 (m, 2H), 1.82–1.90 (m, 1H), 2.22–2.41 (m, 3H), 2.52–2.81 (m, 10H), 3.0–3.20 (m, H), 3.21–3.30 (m, 5H), 3.78 (s, 3H), 6.62–6.72 (m, 2H), 6.82–7.10 (m, 4H), 7.22–7.30 (m, 2H).

**( $\pm$ )-trans-1-[2-[4-(2,3-Dichlorophenyl)piperazin-1-yl]ethyl]-8-methoxy-1,2,3,4,4a,5,10,10a-octahydrobenzo[g]quinoline (34b).** Amide **33b** (130 mg, 0.266 mmol) was reduced using 51 mg (1.33 mmol) of lithium aluminum hydride following procedure C to give solid **34b**, 120 mg (97%).  $^1\text{H}$  NMR (400 MHz,  $\text{CDCl}_3$ )  $\delta$  1.10–1.22 (m, 1H), 1.62–1.77 (m, 2H), 1.83–1.91 (m, 1H), 2.21–2.40 (m, 3H), 2.53–2.80 (m, 10H), 3.1–3.20 (m, H), 3.23–3.32 (m, 5H), 3.78 (s, 3H), 6.63–6.73 (m, 2H), 7.68–7.10 (m, 4H), 7.22–7.30 (m, 2H).

**( $\pm$ )-trans-8-Methoxy-1-[4-(4-phenylpiperazin-1-yl)butyl]-1,2,3,4,4a,5,10,10a-octahydrobenzo[g]quinoline (34c).** Amide **33c** (170 mg, 0.38 mmol) was reduced using 74 mg (1.9 mmol) of lithium aluminum hydride according to procedure C. Column chromatography using EtOAc/MeOH (95:5) gave **34c**, 159 mg (96%).  $^1\text{H}$  NMR (400 MHz,  $\text{CDCl}_3$ )  $\delta$  1.12–1.25 (m, 2H), 1.51–1.73 (m, 6H), 1.84–1.90 (m, 1H), 2.22–2.30 (m, 2H), 2.39–2.41 (m, 3H), 2.58–2.62 (m, 5H), 2.63–2.90 (m, 3H), 2.91–3.11 (m, 1H), 3.14–3.22 (m, 5H), 3.78 (s, 3H), 6.63–6.70 (m, 2H), 6.83–6.86 (t, 1H,  $J = 8$  Hz), 6.92–6.97 (t, 3H,  $J = 8$  Hz), 7.24–7.28 (t, 2H,  $J = 8$  Hz).

**( $\pm$ )-trans-1-[2-(4-Phenylpiperazin-1-yl)ethyl]-1,2,3,4,4a,5,10,10a-octahydrobenzo[g]quinolin-8-ol (35a).** Ether **34a** (100 mg, 0.47 mmol) was demethylated following procedure D. The crude solid was purified by crystallization (EtOAc/MeOH) to give **35a**, 75 mg (78%).  $^1\text{H}$  NMR (400 MHz,  $\text{CDCl}_3$ )  $\delta$  1.12–1.24 (m, 1H), 1.62–1.75 (m, 2H), 1.83–1.92 (m, 1H), 2.24–2.42 (m, 3H), 2.50–2.82 (m, 10H), 3.13–3.20 (m, H), 3.20–3.31 (m, 5H), 6.63–6.74 (m, 2H), 6.83–7.11 (m, 4H), 7.21–7.30 (m, 2H). The free base was then converted to its HCl salt, mp = 167–170 °C. Anal. ( $\text{C}_{25}\text{H}_{33}\text{N}_3\text{O} \cdot 2\text{HCl} \cdot \text{H}_2\text{O}$ ) C, H, N.

**( $\pm$ )-trans-1-[2-[4-(2,3-Dichlorophenyl)piperazin-1-yl]ethyl]-1,2,3,4,4a,5,10,10a-octahydrobenzo[g]quinolin-8-ol (35b).** Ether **34b** (140 mg, 0.30 mmol) was demethylated following procedure D. The crude solid was purified by crystallization (EtOAc/MeOH) to give **35b**, 100 mg (73%).  $^1\text{H}$  NMR (400 MHz,  $\text{CDCl}_3$ )  $\delta$  1.14–1.24 (m, 1H), 1.63–1.79 (m, 2H), 1.84–1.92 (m, 1H), 2.20–2.41 (m, 3H), 2.55–2.83 (m, 10H), 3.2–3.23 (m, H), 3.22–3.34 (m, 5H), 6.60–6.72 (m, 2H), 6.92–7.14 (m, 3H), 7.33–7.40 (m, 1H). The free base was then converted to its HCl salt, mp = 182–185 °C. Anal. ( $\text{C}_{25}\text{H}_{31}\text{Cl}_2\text{N}_3\text{O} \cdot 2\text{HCl}$ ) C, H, N.

**( $\pm$ )-trans-1-[4-(4-Phenylpiperazin-1-yl)butyl]-1,2,3,4,4a,5,10,10a-octahydrobenzo[g]quinolin-8-ol (35c).** Methyl ether **34c** (90 mg, 0.207 mmol) was demethylated according to procedure D to give **35c**, 61 mg (70%), after crystallization from EtOAc/MeOH.  $^1\text{H}$  NMR (400 MHz,  $\text{CDCl}_3$ )  $\delta$  1.112–1.24 (m, 2H), 1.50–1.72 (m, 6H), 1.85–1.90 (m, 1H), 2.21–2.30 (m, 2H), 2.37–2.40 (m, 3H), 2.58–2.63 (m, 5H), 2.62–2.91 (m, 3H), 2.91–3.11 (m, 1H), 3.15–3.23 (m, 5H), 6.62–6.71 (m, 2H), 6.84–6.87 (t, 1H,  $J = 8$  Hz), 6.93–6.98 (t, 3H,  $J = 8$  Hz), 7.24–7.28 (t, 2H,  $J = 8$  Hz). The free base was converted to its HCl salt, mp = 178–183 °C. Anal. ( $\text{C}_{27}\text{H}_{37}\text{N}_3\text{O}$ ) C, H, N.

**( $\pm$ )-trans-2-(7-Methoxy-2,3,4a,5,6,10b-hexahydro-1H-benzo[f]quinolin-4-yl)-1-(4-phenylpiperazin-1-yl)ethanone (37).** This compound was prepared using 200 mg of amine **36**<sup>30</sup> (0.79 mmol), 288 mg of chloride **13a** (0.945 mmol), and 327 mg of  $\text{K}_2\text{CO}_3$  (2.37 mmol) according to procedure B. Column chromatography using EtOAc as eluent afforded **37** 330 mg of ( $\pm$ )-**37** (93%) as an oil.  $^1\text{H}$  NMR ( $\text{CDCl}_3$ )  $\delta$  1.13–1.23 (m, 1H), 1.61–1.76 (m, 2H), 1.82–1.90



(m, 1H), 2.22–2.41 (m, 3H), 2.52–2.81 (m, 10H), 3.0–3.20 (m, H), 3.21–3.30 (m, 5H), 3.78 (s, 3H), 6.62–6.72 (m, 2H), 6.82–7.10 (m, 4H), 7.22–7.30 (m, 2H).

(+)-(4aR,10aR)-trans-2-(7-Methoxy-2,3,4a,5,6,10b-hexahydro-1H-benzof[quinolin-4-yl]-1-(4-phenylpiperazin-1-yl)ethanone ((+)-37). This compound was prepared following procedure B, using 160 mg (0.632 mmol) of the (+)-36<sup>16</sup> isomer (HCl salt) and 166 mg (0.70 mmol) of chloride **13a** to give 260 mg (98%) of (+)-37 as an oil. <sup>1</sup>H NMR (400 MHz, CDCl<sub>3</sub>) δ 1.14–1.24 (m, 1H), 1.63–1.75 (m, 2H), 1.80–1.91 (m, 1H), 2.23–2.41 (m, 3H), 2.51–2.81 (m, 10H), 2.1–3.22 (m, H), 3.20–3.31 (m, 5H), 3.75 (s, 3H), 6.64–6.73 (m, 2H), 6.83–7.12 (m, 4H), 7.21–7.31 (m, 2H).

(-)-(4aS,10bS)-trans-2-(7-Methoxy-2,3,4a,5,6,10b-hexahydro-1H-benzof[quinolin-4-yl]-1-(4-phenylpiperazin-1-yl)ethanone ((-)-37). This compound was prepared following procedure B, using 150 mg (0.632 mmol) of the (-)-36<sup>16</sup> isomer (HCl salt) and 183 mg (0.70 mmol) of chloride **13a** to give 293 mg (96%) of (-)-37 as an oil. <sup>1</sup>H NMR (400 MHz, CDCl<sub>3</sub>) δ 1.15–1.24 (m, 1H), 1.63–1.74 (m, 2H), 1.81–1.92 (m, 1H), 2.23–2.43 (m, 3H), 2.53–2.85 (m, 10H), 3.2–3.26 (m, H), 3.23–3.33 (m, 5H), 3.80 (s, 3H), 6.63–6.70 (m, 2H), 6.81–7.11 (m, 4H), 7.23–7.31 (m, 2H).

(±)-trans-7-Methoxy-4-(2-(4-phenylpiperazin-1-yl)ethyl)-1,2,3,4,4a,5,6,10b-octahydrobenzof[quinoline] (38). Compound **37** (361 mg, 0.833 mmol) was reduced with lithium aluminum hydride (250 mg, 6.66 mmol) according to procedure C to give (±)-38, 335 mg (98%), as an oil, which was sufficiently pure to use in the next step. <sup>1</sup>H NMR (400 MHz, CDCl<sub>3</sub>) δ 1.77–1.82 (m, 2H), 2.17–2.22 (m, 1H), 2.35–2.50 (m, 3H), 2.57–2.75 (m, 8H), 2.94–3.08 (m, 3H), 3.20–3.22 (t, 4H, *J* = 5.2 Hz), 3.81 (s, 3H), 6.69–6.71 (d, 1H, *J* = 8 Hz), 6.83–6.87 (t, 1H, *J* = 8 Hz), 6.92–6.94 (m, 3H), 7.13–7.17 (t, 1H, *J* = 8 Hz), 7.24–7.28 (t, 2H, *J* = 8 Hz).

(+)-(4aR,10aR)-trans-7-Methoxy-4-(2-(4-phenylpiperazin-1-yl)ethyl)-1,2,3,4,4a,5,6,10b-octahydrobenzof[quinoline] ((+)-38). Compound (+)-37 (260 mg, 0.620 mmol) was reduced with lithium aluminum hydride (188 mg, 5.0 mmol) according to procedure C to give (+)-38, 251 mg (99%), as an oil, which was sufficiently pure to use in the next step. <sup>1</sup>H NMR (400 MHz, CDCl<sub>3</sub>) δ 1.75–1.80 (m, 2H), 2.16–2.23 (m, 1H), 2.34–2.51 (m, 3H), 2.58–2.76 (m, 8H), 2.94–3.10 (m, 3H), 3.20–3.22 (t, 4H, *J* = 5.2 Hz), 3.81 (s, 3H), 6.68–6.74 (d, 1H, *J* = 8 Hz), 6.84–6.85 (t, 1H, *J* = 8 Hz), 6.90–6.94 (m, 3H), 7.12–7.18 (t, 1H, *J* = 8 Hz), 7.22–7.29 (t, 2H, *J* = 8 Hz).

(-)-(4aS,10bS)-trans-7-Methoxy-4-(2-(4-phenylpiperazin-1-yl)ethyl)-1,2,3,4,4a,5,6,10b-octahydrobenzof[quinoline] ((-)-38). Compound (-)-37 (293 mg, 0.70 mmol) was reduced with lithium aluminum hydride (212 mg, 5.59 mmol) according to procedure C to give (-)-38, 265 mg (93%), as an oil, which was sufficiently pure to use in the next step. <sup>1</sup>H NMR (400 MHz, CDCl<sub>3</sub>) δ 1.75–1.86 (m, 2H), 2.18–2.26 (m, 1H), 2.34–2.51 (m, 3H), 2.54–2.72 (m, 8H), 2.92–3.06 (m, 3H), 3.22–3.24 (t, 4H, *J* = 5.2 Hz), 3.81 (s, 3H), 6.69–6.70 (d, 1H, *J* = 8 Hz), 6.85–6.89 (t, 1H, *J* = 8 Hz), 6.91–6.95 (m, 3H), 7.12–7.18 (t, 1H, *J* = 8 Hz), 7.23–7.28 (t, 2H, *J* = 8 Hz).

(±)-trans-4-(2-(4-Phenylpiperazin-1-yl)ethyl)-1,2,3,4,4a,5,6,10b-octahydrobenzof[quinolin-7-ol] (8). Compound **38** (335 mg, 0.827 mmol) was demethylated following procedure D. The crude solid was purified by recrystallization (EtOAc/MeOH) to give (±)-8, 264 mg (81%). <sup>1</sup>H NMR (400 MHz, CDCl<sub>3</sub>) δ 1.72–1.70 (m, 2H), 2.11–2.20 (m, 1H), 2.34–2.51 (m, 3H), 2.62–2.79 (m, 8H), 2.96–3.10 (m, 3H), 3.22–3.24 (t, 4H, *J* = 5.2 Hz), 6.70–6.72 (d, 1H, *J* = 8 Hz), 6.81–6.85 (t, 1H, *J* = 8 Hz), 6.94–6.96 (m, 3H), 7.15–7.19 (t, 1H, *J* = 8 Hz), 7.26–7.30 (t, 2H, *J* = 8 Hz). The free base was converted to its HCl salt, mp = 165–169 °C. Anal. (C<sub>25</sub>H<sub>33</sub>N<sub>3</sub>O·2HCl·0.5H<sub>2</sub>O) C, H, N.

(+)-(4aR,10aR)-trans-4-(2-(4-Phenylpiperazin-1-yl)ethyl)-1,2,3,4,4a,5,6,10b-octa-hydrobenzof[quinolin-7-ol] ((+)-8). Compound (+)-38 (250 mg, 0.616 mmol) was demethylated following procedure D. The crude solid was purified by recrystallization

(EtOAc/MeOH) to give (+)-8, 200 mg (82%). [α]<sub>D</sub> +43.6° (c 0.86 in MeOH). <sup>1</sup>H NMR (400 MHz, CDCl<sub>3</sub>) δ 1.71–1.70 (m, 2H), 2.13–2.21 (m, 1H), 2.35–2.53 (m, 3H), 2.60–2.77 (m, 8H), 2.97–3.11 (m, 3H), 3.20–3.22 (t, 4H, *J* = 5.2 Hz), 6.71–6.73 (d, 1H, *J* = 8 Hz), 6.84–6.88 (t, 1H, *J* = 8 Hz), 6.92–6.94 (m, 3H), 7.12–7.20 (t, 1H, *J* = 8 Hz), 7.25–7.31 (t, 2H, *J* = 8 Hz). The free base was converted to its HCl salt, mp = 163–167 °C. Anal. (C<sub>25</sub>H<sub>33</sub>N<sub>3</sub>O·2HCl) C, H, N.

(-)-(4aS,10bS)-trans-4-(2-(4-Phenylpiperazin-1-yl)ethyl)-1,2,3,4,4a,5,6,10b-octa-hydrobenzof[quinolin-7-ol] ((-)-8). Compound (-)-38 (265 mg, 0.653 mmol) was demethylated following procedure D. The crude solid was purified by recrystallization (EtOAc/MeOH) to give (-)-8, 215 mg (84%). [α]<sub>D</sub> -45.6° (c 0.55 in MeOH). <sup>1</sup>H NMR (400 MHz, CDCl<sub>3</sub>) δ 1.71–1.68 (m, 2H), 2.12–2.21 (m, 1H), 2.32–2.49 (m, 3H), 2.61–2.77 (m, 8H), 2.95–3.05 (m, 3H), 3.21–3.23 (t, 4H, *J* = 5.2 Hz), 6.71–6.73 (d, 1H, *J* = 8 Hz), 6.80–6.84 (t, 1H, *J* = 8 Hz), 6.95–6.97 (m, 3H), 7.16–7.20 (t, 1H, *J* = 8 Hz), 7.22–7.26 (t, 2H, *J* = 8 Hz). The free base was converted to its HCl salt, mp = 166–169 °C. Anal. (C<sub>25</sub>H<sub>33</sub>N<sub>3</sub>O·2HCl) C, H, N.

trans-4-Propyl-1,2,3,4,4a,5,6,10b-octahydrobenzof[quinolin-7-ol] (1). To a solution of compound (±)-36 (0.217 g, 1 mmol) and TEA (0.5 mL) in dichloromethane (15 mL) at 0 °C was added propionyl chloride (0.111 g, 1.2 mmol) dropwise. The reaction mixture was allowed to stir for an additional 1 h. The reaction mixture was washed with saturated NaHCO<sub>3</sub> solution, followed by water. The organic layer was dried (Na<sub>2</sub>SO<sub>4</sub>) and the solvent removed in vacuo to yield a viscous liquid (0.2 g) which was subjected to reduction with excess LiAlH<sub>4</sub> following procedure C. Demethylation of the tertiary amine thus obtained was carried out in refluxing aqueous HBr (48%) for 3 h. The acid was removed in vacuo. The residue obtained was converted to free base using aqueous Na<sub>2</sub>CO<sub>3</sub>. The free base was purified using column chromatography (dichloromethane/MeOH 8:2) to yield 187 mg of (±)-1 (92%). <sup>1</sup>H NMR (400 MHz, CDCl<sub>3</sub>) δ 1.04–1.07 (t, 3H, *J* = 8 Hz), 1.46–1.49 (m, 1H), 1.79 (m, 3H), 1.98–2.14 (m, 3H), 2.59–2.77 (m, 3H), 3.03–3.16 (m, 5H), 3.6–3.63 (m, 1H), 6.63–6.65 (d, 1H, *J* = 7.2 Hz), 6.18–6.83 (d, 1H, *J* = 8 Hz), 7.00–7.04 (t, 1H, *J* = 7.2 Hz). The free base was then converted to its oxalate salt, mp = 156–160 °C. Anal. (C<sub>18</sub>H<sub>25</sub>N<sub>3</sub>O<sub>5</sub>) C, H, N.

(±)-trans-2-(6-Methoxy-3,4,4a,5,10,10a-hexahydro-2H-benzof[quinolin-1-yl]-1-(4-phenylpiperazin-1-yl)ethanone (41a). The hydrochloride salt of amine **40**<sup>29</sup> (350 mg, 1.38 mmol), chloride **13a** (383 mg, 1.25 mmol), and K<sub>2</sub>CO<sub>3</sub> (573 mg, 4.15 mmol) in CH<sub>3</sub>CN were reacted following procedure B to yield **41a**, 501 mg (95%), as a yellow oil. <sup>1</sup>H NMR (400 MHz, CDCl<sub>3</sub>) δ 1.62–1.69 (m, 3H), 1.90–1.93 (m, 1H), 2.14–2.36 (m, 4H), 2.65–2.72 (m, 1H), 2.90–2.96 (m, 2H), 3.00–3.12 (m, 3H), 3.17–3.22 (m, 1H), 3.29 (bs, 1H), 3.57–3.60 (m, 1H), 3.69–3.73 (m, 2H), 3.81 (s, 3H), 3.88–3.92 (d, 1H, *J* = 13 Hz), 3.99–4.01 (m, 1H), 6.65–6.67 (d, 1H, *J* = 8 Hz), 6.70–6.72 (d, 1H, *J* = 8 Hz), 6.88–6.95 (m, 3H), 7.07–7.11 (t, 1H, *J* = 8 Hz), 7.23–7.31 (m, 2H).

(±)-trans-1-[4-(2,3-Dichlorophenyl)piperazin-1-yl]-2-(6-methoxy-3,4,4a,5,10,10a-hexahydro-2H-benzof[quinolin-1-yl]ethanone (41b). The hydrochloride salt of amine **40** (100 mg, 0.386 mmol), chloride **13b** (118 mg, 0.386 mmol), and K<sub>2</sub>CO<sub>3</sub> (106 mg, 0.772 mmol) in CH<sub>3</sub>CN were reacted following procedure B to yield **41b**, 170 mg (90%), as an oil, which was used without further purification. <sup>1</sup>H NMR (400 MHz, CDCl<sub>3</sub>) δ 1.61–1.68 (m, 3H), 1.91–1.94 (m, 1H), 2.13–2.35 (m, 4H), 2.66–2.73 (m, 1H), 2.91–2.97 (m, 2H), 3.01–3.13 (m, 3H), 3.17–3.22 (m, 1H), 3.29 (bs, 1H), 3.57–3.60 (m, 1H), 3.69–3.73 (m, 2H), 3.81 (s, 3H), 3.88–3.92 (d, 1H, *J* = 13 Hz), 3.99–4.01 (m, 1H), 6.58–6.59 (d, 1H, *J* = 8 Hz), 6.63–6.65 (d, 1H, *J* = 8 Hz), 6.85–6.84 (d, 1H, *J* = 8 Hz), 7.00–7.04 (t, 1H, *J* = 8 Hz), 7.07–7.13 (m, 2H).

(±)-trans-6-Methoxy-1-[2-(4-phenylpiperazin-1-yl)ethyl]-1,2,3,4,4a,5,10,10a-octahydrobenzof[quinoline] (42a). Amide **41a** (500 mg, 1.38 mmol) was reduced with lithium aluminum hydride (280 mg, 7.0 mmol) following procedure C to give **52**, 480 mg (99%) of **42a**, which was used without further purification. <sup>1</sup>H NMR (400 MHz, CDCl<sub>3</sub>) δ 1.60–1.72 (m, 4H), 2.21–2.27 (m, 2H),



1.90–1.94 (m, 1H), 2.59–2.74 (m, 8H), 2.33–2.39 (m, 1H), 2.91–3.09 (m, 3H), 3.22–3.27 (m, 5H), 3.81 (s, 3H), 6.65–6.67 (d, 1H,  $J = 8$  Hz), 6.70–6.72 (d, 1H,  $J = 8$  Hz), 6.88–6.95 (m, 3H), 7.07–7.11 (t, 1H,  $J = 8$  Hz), 7.23–7.31 (m, 2H).

(±)-**trans-1-a{2-[4-(2,3-Dichlorophenyl)piperazin-1-yl]ethyl}-6-methoxy-1,2,3,4,4a-5,10,10a-octahydrobenzo[g]quinoline (42b)**. Amide **41b** (170 mg, 0.349 mmol) was reduced with lithium aluminum hydride (55 mg, 1.43 mmol) following procedure C to give **42b**, 152 mg (92%) of the titled product, which was used without further purification. <sup>1</sup>H NMR (400 MHz, CDCl<sub>3</sub>)  $\delta$  1.59–1.66 (m, 3H), 1.90–1.93 (m, 1H), 2.11–2.33 (m, 4H), 2.64–2.71 (m, 1H), 2.90–2.96 (m, 2H), 3.00–3.12 (m, 3H), 3.12–3.29 (m, 8H), 3.81 (s, 3H), 6.58–6.59 (d, 1H,  $J = 8$  Hz), 6.63–6.65 (d, 1H,  $J = 8$  Hz), 6.85–6.84 (d, 1H,  $J = 8$  Hz), 7.00–7.04 (t, 1H,  $J = 8$  Hz), 7.07–7.13 (m, 2H).

(±)-**trans-1-[2-(4-Phenylpiperazin-1-yl)ethyl]-1,2,3,4,4a,5,10,10a-octahydrobenzo[g]quinolin-6-ol (43a)**. Compound **42a** (470 mg, 1.16 mmol) was demethylated following procedure D. The crude solid was purified by column chromatography (1:10 MeOH/EtOAc) to give **43a**, 400 mg (88%). <sup>1</sup>H NMR (400 MHz, CDCl<sub>3</sub>)  $\delta$  1.13–1.15 (m, 2H), 1.90–1.92 (m, 1H), 2.15–2.27 (m, 3H), 2.33–2.39 (m, 1H), 2.60–2.75 (m, 9H), 2.85–2.91 (m, 1H), 3.03–3.11 (m, 2H), 3.17–3.23 (m, 5H), 6.53–6.55 (d, 1H,  $J = 7.6$  Hz), 6.64–6.66 (d, 1H,  $J = 8$  Hz), 7.24–7.28 (t, 2H,  $J = 8$  Hz), 6.83–6.87 (t, 1H,  $J = 8$  Hz), 6.91–6.99 (m, 3H). The free base was then converted to its HCl salt, mp = 174–179 °C. Anal. (C<sub>25</sub>H<sub>33</sub>N<sub>3</sub>O·3HCl) C, H, N.

(±)-**trans-1-[2-[4-(2,3-Dichlorophenyl)piperazin-1-yl]ethyl]-1,2,3,4,4a,5,10,10a-octahydrobenzo[g]quinolin-6-ol (43b)**. Compound **42b** (152 mg, 0.321 mmol) was demethylated following procedure D. The crude solid was purified by column chromatography (1:10 MeOH/EtOAc) to give **43b**, 102 mg (69%). <sup>1</sup>H NMR (400 MHz, CDCl<sub>3</sub>)  $\delta$  1.12–1.25 (m, 2H), 1.82–1.91 (m, 1H), 2.21–2.42 (m, 3H), 2.51–2.63 (m, 9H), 2.78–2.81 (m, 1H), 2.98–3.12 (m, 8H), 6.53–6.54 (d, 1H,  $J = 8$  Hz), 6.58–6.60 (d, 1H,  $J = 8$  Hz), 6.80–6.79 (d, 1H,  $J = 8$  Hz), 6.95–7.00 (t, 1H,  $J = 8$  Hz), 7.02–7.09 (m, 2H). The free base was then converted to its HCl salt, mp = 161–165 °C. Anal. (C<sub>25</sub>H<sub>31</sub>N<sub>3</sub>OCl<sub>2</sub>·2HCl) C, H, N.

(±)-**trans-1-Propyl-1,2,3,4,4a,5,10,10a-octahydrobenzo[g]quinolin-6-ol (2)**. To a solution of compound (±)-**40** (0.217 g, 1 mmol) and TEA (0.5 mL) in dichloromethane (15 mL) at 0 °C was added propionyl chloride (0.111 g, 1.2 mmol) dropwise. The reaction mixture was allowed to stir for an additional 1 h. The reaction mixture was washed with saturated NaHCO<sub>3</sub> solution, followed by water. The organic layer was dried (Na<sub>2</sub>SO<sub>4</sub>) and the solvent removed in vacuo to yield a thick oil (0.2 g), which was subjected to reduction with excess LiAlH<sub>4</sub> following procedure C. Demethylation of the tertiary amine thus obtained was carried out in refluxing aqueous HBr (48%) for 3 h. The acid was removed in vacuo. The residue obtained was converted to free base using aqueous Na<sub>2</sub>CO<sub>3</sub>. The free base was purified using column chromatography (dichloromethane/MeOH 8:2) to give 0.1 g of **2**. The purified free base was converted to the HCl salt. <sup>1</sup>H NMR (400 MHz, CD<sub>3</sub>OD):  $\delta$  1.0–1.04 (t, 3H), 1.45–1.51 (m, 2H), 1.67–1.86 (m, 5H), 1.91–1.94 (m, 1H), 2.10–2.16 (m, 1H), 2.74–2.78 (m, 2H), 2.89–3.04 (m, 5H), 6.52–6.55 (m, 2H), 6.85–6.89 (m, 1H). The free base was converted to HCl salt, mp = 165–167 °C. Anal. (C<sub>16</sub>H<sub>25</sub>ClNO·HCl·0.3C<sub>2</sub>H<sub>5</sub>OC<sub>2</sub>H<sub>5</sub>) C, H, N.

**Molecular Modeling.** All molecular modeling studies reported herein were performed on a Hewlett-Packard xw4300 computer workstation with main memory of 2 GB and Intel Pentium 4 CPU of 3.4 GHz running under the operating system Linux Red Hat 3. The molecular modeling software packages Sybyl 7.1<sup>32</sup> and Molecular Operating Environment (MOE) 2007.09<sup>33</sup> were employed for the present work.

The structures used in the present study were constructed either from X-ray crystal structure or using fragments in Sybyl's fragment library. All the structures were generated in their N-protonated forms. Partial atomic charges were calculated using Gasteiger–Hückel method in Sybyl 7.1. Each structure was fully geometry-optimized using the Tripos force field<sup>34</sup> with a distance-dependent dielectric

function until a root-mean-square (rms) deviation of 0.001 kcal/(mol Å) was achieved. Ring conformations of bi- and tricyclic aminotetralin derivatives were generated using simulated annealing protocol with default settings (no. of cycles, 10; heating, 700 K for 1000 fs; annealing, 50 K for 1000 fs; annealing function, exponential) in Sybyl 7.1. The minimum energy conformations for each of the bi- and tricyclic ring systems were further minimized in Sybyl using the settings mentioned above. Further, rotatable bonds in all molecules were searched from 0 to 359° in 10° increments using systematic search protocol in Sybyl. The minimum energy conformations were minimized further as described above. The molecules were imported in TriposMol2 (.mol2) format in MOE 2007.09 and stored in a molecular database. This database was used as an input in the Pharmacophore Elucidation functionality in MOE. The structures of molecules used for generating pharmacophore queries are shown Figures 1 and 3.

The objective of Pharmacophore Elucidation is to generate all popular pharmacophore queries (with coverage  $n$ , typically 90% of all active molecules) considering all possible discrete geometries with all possible combinations of input query expressions. The Pharmacophore Elucidator operates on 3D conformations of the molecules present in the input database. In the present study the Conformations option in Pharmacophore Elucidation panel was set to bond rotation wherein the rotatable bonds of each molecule were set systematically to specific torsion angles from a collection of rules. The ring conformations were not searched. The default annotation scheme CHD was used for determining the pharmacophore features of each molecule. Pharmacophore Elucidator generates pharmacophores compatible with the specified scheme. Other parameter values in the Pharmacophore Elucidation panel were kept at their default values. The alignment options (emphasize aromatic atoms and emphasize donor and acceptor atoms) that influence the overlap scoring were enabled. The results of the pharmacophore generation were written to an output database, which was analyzed further to select appropriate pharmacophore hypothesis.

The set of compounds used for pharmacophore generation consisted of conformationally constrained (bi- and tricyclic aminotetralin derivatives) structures shown in Figure 3 with their dopamine D2 and D3 receptor binding affinities listed in Table 1. To determine the appropriate annotation scheme, several runs with other annotation schemes given in Pharmacophore Elucidation functionality such as PCH, CHD, PCHD, PPCH, PCHD, Unified, etc. were tried, keeping all other parameters constant (data not shown). For these initial trial runs, compounds *R*-(+)-7-OH-DPAT, *S*-(-)-5-OH-DPAT, and *R*-(+)-**5**, known D2/D3 agonists, were used. It is well-known from earlier dopamine pharmacophores that an aromatic H-bond donor and cationic nitrogen (reinforced H-bonding) are necessary to interact with dopamine receptor serine and aspartate residues, respectively.<sup>15</sup> To include these highly directional pharmacophore requirements such as reinforced H-bonding, the annotation scheme CHD was selected. This scheme avoids use of atomic H-bond/acceptor features but includes the directional character of the atomic H-bond donor/acceptor features. This is particularly useful for DA ligands, since these possess varying nature of the H-bond donor, which interacts with serine. Also, enabling the alignment options emphasize aromatic atoms and emphasize donor and acceptor atoms led to meaningful pharmacophore hypotheses. The final pharmacophores were generated using the CHD annotation scheme with above-mentioned alignment options. For the generation of pharmacophore hypotheses based on hybrid analogues, compounds (+)-**6**, (-)-**7**, (-)-**8** (4aS, 10bS), and (-)-**11** (*S*-enantiomer) were used. Selection of the appropriate hypotheses was based on overall alignment score and the associated pharmacophore features.

**Measurement of Affinity in Inhibiting [<sup>3</sup>H]Spiperone Binding to Dopamine D2 and D3 Receptors.** Binding affinities were assessed according to the general procedure described in our previous study.<sup>22</sup> Briefly, membranes from HEK 293 cells expressing rat D2L and D3 receptors were incubated with each test compound and [<sup>3</sup>H]spiperone (0.4 nM, 15 Ci/mmol, Perkin-Elmer) for 1 h at 30 °C in 50 mM Tris-HCl (pH 7.4), with 0.9% NaCl, and 0.025% ascorbic acid in the absence of GTP. (+)-Butaclamol (2 M) was used to define nonspecific binding. Assays were



terminated by addition of ice-cold buffer and filtration in the MACH 3-96 Tomtec harvester (Wallac, Gaithersburg, MD). IC<sub>50</sub> values were estimated by nonlinear regression analysis with the logistic model in the least-squares fitting program ORIGIN and converted to inhibition constants (*K<sub>i</sub>*) by the Cheng–Prusoff equation.<sup>35</sup> In this conversion, the *K<sub>d</sub>* values for [<sup>3</sup>H]spiperone binding were 0.057 nM for D2 receptors and 0.125 nM for D3 receptors.

**Acknowledgment.** This work is supported by National Institute of Neurological Disorders and Stroke/National Institutes of Health (Grant NS047198, A.K.D.). We thank Drs. Swati Biswas and Fernando Fernandez for synthesizing compounds (+)-**6** and **9**. We are grateful to Dr. K. Neve, Oregon Health and Science University, Portland, OR, for D2L and D3 expressing HEK cells.

**Supporting Information Available:** Elemental analysis data for all final targets and additional synthesis information and analytical data. This material is available free of charge via the Internet at <http://pubs.acs.org>.

## References

- (1) Emilien, G.; Maloteaux, J.-M.; Geurts, M.; Hoogenberg, K.; Cragg, S. Dopamine receptors. Physiological understanding to therapeutic intervention potential. *Pharmacol. Ther.* **1999**, *84*, 133–156.
- (2) Missale, C.; Nash, S. R.; Robinson, S. W.; Jaber, M.; Caron, M. G. Dopamine receptors: from structure to function. *Physiol. Rev.* **1998**, *78*, 189–225.
- (3) D'Ischia, M.; Protá, G. Biosynthesis, structure, and function of neuromelanin and its relation to Parkinson's disease: a critical update. *Pigm. Cell Res.* **1997**, *10*, 370–376.
- (4) Gurevich, E. V.; Joyce, J. N. Distribution of dopamine D<sub>3</sub> receptor expressing neurons in the human forebrain: comparison with D<sub>2</sub> receptor expressing neurons. *Neuropsychopharmacology* **1999**, *20*, 60–80.
- (5) Boeckler, F.; Gmeiner, P. The structural evolution of dopamine D<sub>3</sub> receptor ligands: structure–activity relationships and selected neuropharmacological aspects. *Pharmacol. Ther.* **2006**, *112*, 281–333.
- (6) McDermed, J. D.; McKenzie, G. M.; Freeman, H. S. Synthesis and dopaminergic activity of (±)-, (+)-, and (–)-2-dipropylamino-5-hydroxy-1,2,3,4-tetrahydronaphthalene. *J. Med. Chem.* **1976**, *19*, 547–549.
- (7) Tedesco, J. L.; Seeman, P.; McDermed, J. D. The conformation of dopamine at its receptor: binding of monohydroxy-2-aminotetralin enantiomers and positional isomers. *Mol. Pharmacol.* **1979**, *16*, 369–381.
- (8) Cannon, J. G.; Lee, T.; Goldman, H. D.; Costall, B.; Naylor, R. J. Cerebral dopamine agonist properties of some 2-aminotetralin derivatives after peripheral and intracerebral administration. *J. Med. Chem.* **1977**, *20*, 1111–1116.
- (9) McDermed, J. D.; McKenzie, G. M.; Phillips, A. P. Synthesis and pharmacology of some 2-aminotetralins. Dopamine receptor agonists. *J. Med. Chem.* **1975**, *18*, 362–367.
- (10) Hacksell, U.; Svensson, U.; Nilsson, J. L. G.; Hjorth, S.; Carlsson, A.; Wikström, H.; Lindberg, P.; Sanchez, D. N-Alkylated 2-aminotetralins: central dopamine-receptor stimulating activity. *J. Med. Chem.* **1979**, *22*, 1469–1475.
- (11) Damsma, G.; Bottema, T.; Westerink, B. H.; Tepper, P. G.; Dijkstra, D.; Pugsley, T. A.; MacKenzie, R. G.; Heffner, T. G.; Wikström, H. Pharmacological aspects of R-(+)-7-OH-DPAT, a putative dopamine D<sub>3</sub> receptor ligand. *Eur. J. Pharmacol.* **1993**, *249*, R9–R10.
- (12) Cox, B. A.; Henningsen, R. A.; Spanoyannis, A.; Neve, R. L.; Neve, K. A. Contributions of conserved serine residues to the interactions of ligands with dopamine D<sub>2</sub> receptors. *J. Neurochem.* **1992**, *59*, 627–635.
- (13) Sartania, N.; Strange, P. G. Role of conserved serine residues in the interaction of agonists with D<sub>3</sub> dopamine receptors. *J. Neurochem.* **1999**, *72*, 2621–2624.
- (14) Lundstrom, K.; Turpin, M. P.; Large, C.; Robertson, G.; Thomas, P.; Lewell, X. Q. Mapping of dopamine D<sub>3</sub> receptor binding site by pharmacological characterization of mutants expressed in CHO cells with the Semliki Forest virus system. *J. Recept. Signal Transduction Res.* **1998**, *18*, 133–150.
- (15) Seiler, M. P.; Markstein, R.; Walkinshaw, M. D.; Boelsterli, J. J. Characterization of dopamine receptor subtypes by comparative structure–activity relationships: dopaminomimetic activities and solid state conformation of monohydroxy-1,2,3,4,4a,5,10,10a-octahydrobenzo[g]quinolines and its implications for a rotamer-based dopamine receptor model. *Mol. Pharmacol.* **1989**, *35*, 643–651.
- (16) Wikström, H.; Andersson, B.; Sanchez, D.; Lindberg, P.; Arvidsson, L. E.; Johansson, A. M.; Nilsson, J. L.; Svensson, K.; Hjorth, S.; Carlsson, A. Resolved monophenolic 2-aminotetralins and 1,2,3,4,4a,5,6,10b-octahydrobenzo[f]quinolines: structural and stereochemical considerations for centrally acting pre- and postsynaptic dopamine-receptor agonists. *J. Med. Chem.* **1985**, *28*, 215–225.
- (17) (a) Wikström, H.; Andersson, B.; Elebring, T.; Svensson, K.; Carlsson, A.; Largent, B. N-Substituted 1,2,3,4,4a,5,6,10b-octahydrobenzo[f]quinolines and 3-phenylpiperidines: effects on central dopamine and  $\sigma$  receptors. *J. Med. Chem.* **1987**, *30*, 2169–2174. (b) Witkin, J. M.; Levant, B.; Zapata, A.; Kaminski, R.; Gasior, M. The dopamine D<sub>3</sub>/D<sub>2</sub> agonist (+)-PD-128,907 [(R-(+)-trans-3,4a,10b-tetrahydro-4-propyl-2H,5H-1-benzopyrano-[4,3-b]-1,4-oxazin-9-ol)] protects against acute and cocaine-kindled seizures in mice: further evidence for the involvement of D<sub>3</sub> receptors. *J. Pharmacol. Exper. Ther.* **2008**, *326*, 930–938.
- (18) Cannon, J. G.; Hamer, R. L.; Ilhan, M.; Bhatnagar, R. K.; Long, J. P. Conformationally restricted congeners of dopamine derived from octahydrobenzo[g]quinoline and octahydrobenzo[f]quinoline. *J. Med. Chem.* **1984**, *27*, 190–195.
- (19) Wikström, H.; Sanchez, D.; Lindberg, P.; Arvidsson, L.-E.; Hacksell, U.; Johansson, A.; Nilsson, J. L. G.; Hjorth, S.; Carlsson, A. Monophenolic octahydro-benzo[f]quinolines: central dopamine- and serotonin-receptor stimulating activity. *J. Med. Chem.* **1982**, *25*, 925–931.
- (20) Dutta, A. K.; Fei, X.-S.; Reith, M. E. A. A novel series of hybrid compounds derived by combining 2-aminotetralin and piperazine fragments: binding activity at D<sub>2</sub> and D<sub>3</sub> receptors. *Bioorg. Med. Chem. Lett.* **2002**, *12*, 619–622.
- (21) Dutta, A. K.; Venkataraman, S. K.; Fei, X.-S.; Kolhatkar, R.; Zhang, S.; Reith, M. E. A. Synthesis and biological characterization of novel hybrid 7-[[2-(4-phenylpiperazin-1-yl)ethyl]-propylamino]-5,6,7,8-tetrahydronaphthalen-2-ol and their heterocyclic bioisosteric analogues for dopamine D<sub>2</sub> and D<sub>3</sub> receptors. *Bioorg. Med. Chem.* **2004**, *12*, 4361–4373.
- (22) Biswas, S.; Zhang, S.; Fernandez, F.; Ghosh, B.; Zhen, J.; Kuzhikandathil, E.; Reith, M. E. A.; Dutta, A. K. Further structure–activity relationships study of hybrid 7-[[2-(4-phenylpiperazin-1-yl)ethyl]-propylamino]-5,6,7,8-tetrahydronaphthalen-2-ol analogues: identification of a high-affinity D<sub>3</sub>-preferring agonist with potent in vivo activity with long duration of action. *J. Med. Chem.* **2008**, *51*, 101–117.
- (23) Biswas, S.; Hazeldine, S.; Ghosh, B.; Parrington, I.; Kuzhikandathil, E.; Reith, M. E.; Dutta, A. K. Bioisosteric heterocyclic versions of 7-[[2-(4-phenylpiperazin-1-yl)ethyl]propylamino]-5,6,7,8-tetrahydronaphthalen-2-ol: identification of highly potent and selective agonists for dopamine D<sub>3</sub> receptor with potent in vivo activity. *J. Med. Chem.* **2008**, *51*, 3005–3019.
- (24) Beres, J. A.; Cannon, J. G. Regiospecific carboxylation of certain methoxylated 2-tetralones. *Synth. Commun.* **1979**, *9*, 819–824.
- (25) Khatib, S.; Tal, S.; Godsi, O.; Peskin, U.; Eichen, Y. Site selective processes: a combined theoretical and experimental investigation of thermally activated tautomerization processes in 2-(2,4-dinitrobenzyl)pyridine derivatives. *Tetrahedron* **2000**, *56*, 6753–6761.
- (26) Walsh, D. A.; Smisman, E. E. Observable magnetic nonequivalence of diastereotopic protons as a stereochemical probe. *J. Org. Chem.* **1974**, *39*, 3705–3708.
- (27) Xia, Y.; Reddy, E. R.; Kozikowski, A. P. Synthesis of the benzenoid analogue of the Chinese nootropic agent huperzine A. *Tetrahedron Lett.* **1989**, *30*, 3291–3294.
- (28) Cannon, J.; Chang, Y.-a.; Amoo, V.; Walker, K. Stereospecific route to trans-1,2,3,4,4a-5,6,10b-octahydrobenzo[f]quinolines. *Synthesis* **1986**, 494–496.
- (29) Mellin, C.; Hacksell, U. Stereoselective synthesis of methoxy substituted 1,2,3,4,4a-5,10,10a-octahydrobenzo[g]quinolines. *Tetrahedron* **1987**, *43*, 5443–5450.
- (30) ten Hoeve, W.; Wynberg, H. The design of resolving agents. Chiral cyclic phosphoric acids. *J. Org. Chem.* **1985**, *50*, 4508–4514.
- (31) Varady, J.; Wu, X.; Fang, X.; Min, J.; Hu, Z.; Levant, B.; Wang, S. Molecular modeling of the three-dimensional structure of dopamine 3 (D<sub>3</sub>) subtype receptor: discovery of novel and potent D<sub>3</sub> ligands through a hybrid pharmacophore- and structure-based database searching approach. *J. Med. Chem.* **2003**, *46*, 4377–4392.
- (32) SYBYL Molecular Modeling System, version 7.1; Tripos Inc., St. Louis, MO 63144-2913.
- (33) Molecular Operating Environment (MOE) 2007.09 is available from Chemical Computing Group, Inc., 1010 Sherbrooke Street W, Suite 910, Montreal, Quebec H3A 2R7, Canada.
- (34) Clark, M.; Cramer, R. D., III; Van Opdenbosh, N. Validation of the general purpose Tripos 5.2 force field. *J. Comput. Chem.* **1989**, *10*, 982–1012.
- (35) Cheng, Y.; Prusoff, W. H. Relationship between the inhibition constant (*K<sub>i</sub>*) and the concentration of inhibitor which causes 50% inhibition (*I*<sub>50</sub>) of an enzymatic reaction. *Biochem. Pharmacol.* **1973**, *22*, 3099–3108.